

DEPARTMENT OF THE INTERIOR

U.S. GEOLOGICAL SURVEY

**Cruise Report,**  
**Hawaiian GLORIA Legs 3 and 4**  
**F3-88-HW and F4-88-HW**

by

William R. Normark<sup>1</sup>, Robin T. Holcomb<sup>2</sup>, Roger C. Searle<sup>3</sup>, Michael L. Somers<sup>3</sup>, and  
Christina E. Gutmacher<sup>1</sup>

Open-File Report 89-213

<sup>1</sup>U.S. Geological Survey, Menlo Park, California

<sup>2</sup>U.S. Geological Survey, Seattle, Washington

<sup>3</sup>Institute of Oceanographic Sciences Deacon Laboratory, Wormley, United Kingdom

This report is preliminary and has not been reviewed for conformity with U.S. Geological Survey editorial standards or with the North American Stratigraphic Code. Any use of trade, product, or firm names is for descriptive purposes only and does not imply endorsement by the U.S. Government.

## INTRODUCTION

This cruise was the third of a multi-year program to survey the Hawaiian Ridge Exclusive Economic Zone (EEZ) using the Geologic Long Range Inclined ASDIC (GLORIA; note: ASDIC refers to side-scan sonar under the acronym Anti-Submarine Detection Information Committee; Somers et al., 1978) and was carried out between 11 March and 5 April 1988 (Julian days 071 to 096). The objective is to produce an atlas that displays geologic and morphologic characters of the seafloor as a first step toward evaluation of the economic potential and other possible uses of the EEZ. The Hawaiian Ridge is the fifth major segment of the U.S. EEZ in which GLORIA studies have been initiated; the others are: the western U.S. off Washington, Oregon, and California; the Gulf of Mexico and Caribbean; the Atlantic margin of the East Coast; and the Bering Sea-Aleutian-southwestern Alaskan margin. At this time, only the West Coast and Gulf of Mexico survey data are complete and published in atlas form (EEZ SCAN 84 Scientific Staff, 1986 ; and EEZ SCAN 85 Scientific Staff, 1987).

The initial Hawaiian Ridge atlas will require approximately one-half year of GLORIA surveying. At the present time, the survey effort for this atlas is expected to be completed by early October 1988, and the area covered will extend from the southeastern end of the Hawaiian Ridge EEZ to about longitude 163° W (250 km west of the island of Kauai; refer to Figure 1). As tentatively scheduled, the Hawaiian Ridge effort would extend through 1990 with surveying continuing westward .

Leg 1 of the Hawaiian Ridge survey was conducted from 13 October to 3 November 1986 (Holmes et al., 1987) and Leg 2 was done from 5 November to 26 November 1986 (Normark et al., 1987). Those surveys covered the EEZ surrounding the Island of Hawaii at the southeastern end of the Hawaiian chain. In addition to the GLORIA data, standard cruise operations include: seismic-reflection profiling using an air-gun sound source, 3.5-kHz high-resolution profiling, 10-kHz echo-sounding, magnetic and gravity potential-field measurements, and upper water-column temperature profiles using expendable bathythermographs.

GLORIA imaging cruises are followed by ground-truth cruises in which particularly important features imaged by GLORIA are investigated further using methods that cannot be used while an imaging cruise is in progress. The initial ground-truth cruise in the Hawaiian EEZ was conducted from 25 February to 9 March 1988; it was focused on volcanic features close to the Island of Hawaii and employed dredging, seafloor photography, box coring, and magnetic measurements (Clague et al., 1988).

## OPERATIONS

The GLORIA surveys are conducted from the R/V FARNELLA, a converted freezer trawler under lease to U.S. Geological Survey through the Institute of Oceanographic Sciences (IOS) in Wormley, England. The FARNELLA arrived in Hilo, Hawaii, on 9 March at the end of the initial ground-truth cruise by USGS personnel. During two days in Hilo there was a partial changeover of USGS personnel, who were joined by the IOS party responsible for final preparation and operation of the GLORIA system. The normal scientific party was augmented for the short (5-day) leg 3 operation by 5 administrators of the U.S. Department of Interior and Geological Survey, who acted as watchstanders during the cruise and by a senior official of J. Marr, the owner/operator of the FARNELLA. A training session for the 5 temporary watchstanders was given prior to sailing on 11 March to smooth their transition to shipboard activities.

The GLORIA surveying responsibilities are split between IOS and USGS personnel. The IOS participants are responsible for all operations involving GLORIA, as well as for all deck

operations, maintenance of the air-gun seismic-reflection system and the 3.5- and 10-kHz profiling systems, and logging and final processing of navigation data. The USGS personnel are responsible for real-time navigation and all aspects of the gravimeter and gradiometer operations and for watchstanding duties for everything except the GLORIA system. The co-chief scientists from the USGS and IOS are jointly responsible for general survey planning and construction of two sets of field mosaics of the GLORIA data.

The tabulations below review the scientific personnel, the schedule of field operations, and the status of equipment throughout the legs 3 and 4 operations.

### **Scientific Party for F3-88-HW (Leg 3)**

#### U.S. Geological Survey

Gann, John	Navigator
Gilbert, Charles	Geologist/navigator
Holcomb, Robin	Co-chief scientist
Kooker, Lawrence	Electronics technician
Normark, William	Co-chief scientist
Pickthorn, Ledabeth	Navigator/DAFE

#### Institute of Oceanographic Sciences, United Kingdom

Harris, Andrew	Electronics technician
Searle, Roger	Co-chief scientist
Somers, Michael	GLORIA supervisor
Whittle, Steve	Mechanical technician
Woodward, Emma	Geologist/photographer

#### Natural Environment Research Council/Research Vessel Services (U.K.)

Knight, Gareth	Computer support
----------------	------------------

#### Visiting Scientist (Colorado State University)

Garcia, Brenda	Geologist
----------------	-----------

#### Executive Guests

Frederick, Doyle	Associate Director, USGS
Hill, Gary	Chief, Office of Energy and Marine Geol., USGS
Hind, James	Director, J.Marr (Shipping), Ltd.
Morgan, Benjamin	Chief Geologist, USGS
Saunders, Theodore	Office of the Director, USGS
Ziglar, James	Assistant Secretary, Department of Interior

## Scientific Party for F4-88-HW (Leg 4)

### U.S. Geological Survey

Gilbert, Charles	Geologist/navigator
Holcomb, Robin	Co-chief scientist
Kooker, Lawrence	Electronics technician
Normark, William	Co-chief scientist
Pickthorn, Ledabeth	Navigator/DAFE

### Institute of Oceanographic Sciences, United Kingdom

Harris, Andrew	Electronics technician
Searle, Roger	Co-chief scientist
Somers, Michael	GLORIA supervisor
Whittle, Steve	Mechanical technician
Woodward, Emma	Geologist/photographer

### Natural Environment Research Council/Research Vessel Services (U.K.)

Lloyd, Robert	Computer support
---------------	------------------

### Visiting Scientist (Colorado State University)

Garcia, Brenda	Geologist
----------------	-----------

### Living Tapes (UK)

Chilcott, Martin	Film director
Rosenberg, John	Cameraman
Michaels, Mike	Soundman

The latter group, a video production company invited by Tony Laughton (IOS), is filming a documentary on the GLORIA program in the U.S. EEZ, tentatively titled "Sounding the Deep", which is one of a series for UK Channel 4 TV on oceanography to be called "Oceans of Wealth." These folks left the FARNELLA off northeast Oahu via water taxi on 080/0100.

### **Schedule of Field Operations, F3-88-HW**

The following list is an abbreviated summary of the survey operations. Each entry begins with day of the year/Greenwich Mean Time (GMT) for the starting point of each survey segment. Figure 2 shows the tracklines for this leg. In the following review of field operations, including accompanying tables and appendices, the term "pass" refers to an interval of time (generally six hours) for recording GLORIA data that is limited by the digital taping procedure. The term "line" refers to track segments, which ideally are straight segments; changes in line numbers, which are consecutive from the start of the cruise, generally reflect course changes exceeding 10<sup>o</sup> (approximately). Thus, operations referenced to line numbers are those systems independent of the GLORIA recording system. For conversion to local time, note that day 071 is March 11 and that local Hawaiian time is 10 hours behind GMT, e.g., 1900 GMT is 0900 local.

1. 071/1930 Depart Hilo, Hawaii.
2. 071/2020 Slow to deploy the 3.5- and 10-kHz tow vehicles. Equipment problems delay deployment of remaining gear until 072/0413.
3. 072/0948 Begin pass 1 on logging GLORIA with normal underway watchkeeping; all gear deployed and operational, if not ideally so (see Equipment Review). As each system came on line, logging started to allow the temporary watchstanders to become familiar with underway procedures.
4. 072/1030 End line "0" to begin official survey. Start line 1, a northerly traverse across several lines from F5-86-HW toward the endpoint of that survey to finish the outer part of the EEZ area and to provide further navigational constraints for the earlier lines, which were poorly located because of inadequate navigational data.
5. 076/1520 End of line 9 and end of watchstanding for F3; gear pulled for short transit to Honolulu.

### **Schedule of Field Operations, F4-88-HW**

The first two days of field operations during this leg reflect the presence of the camera crew from Living Tapes (UK). The operational area along the flank of the Hawaiian Ridge along Maui, Molokai, and Oahu was selected in part because the film crew was to be transferred to a shore boat within 20 nm of Oahu at the end of two days of filming. In addition, the deployment of GLORIA itself was later than necessary to allow filming of the launch sequence several times from different vantage points. Both of these initial constraints were further complicated when it became clear during the launch that the hydraulic system in the cradle assembly was not fully operational. Figure 3 shows the tracklines for this leg.

1. 077/2120 Depart Honolulu, Hawaii approximately two and a half hours late as a result of attempted repairs to the GLORIA cradle hydraulic system.
2. 077/2256 Slow to launch the 3.5-kHz and 10-kHz tow fish. Begin filming segments of GLORIA launch operations.
3. 078/0201 Begin actual launch sequence for GLORIA, air gun, streamer, and magnetometer.
4. 078/0249 Begin pass 1 for logging GLORIA.
5. 078/0336 Start line 001. All systems operational; the 3.5 kHz and air gun profiles are generally improved over leg F3 operations; see equipment logs that follow.
6. 079/2108 End line 010 to prepare for transfer of the movie/TV folks to a water taxi. The FARNELLA proceeded to a point near the end of line 009 as arranged earlier, and the transfer took place on time at 080/0100. By 0120, we were underway and streaming gear in preparation to resume survey operations (Figure 3).
7. 080/0146 Start line 011. Lines 011 to 013 are mostly redundant but will provide a new view of the slide off Molokai on our way to resume the deep-water line started during the port-bound track at the end of F3.
8. 080/0959 Start line 014 to begin main body of survey activity on deep-water lines subparallel to the Hawaiian Ridge.
9. 093/0307 End line 25, which completes the outer EEZ boundary for both the F5-86 leg and this one. Commence a traverse to the south across the main grid to finish the northwestern part of line 13 and to do the slope northwest of Oahu.
10. 095/0959 End line 36, which completes the survey of northwestern slope of Oahu. Begin traverse to recon possible slides south of Kauai until end of survey.
11. 095/2237 End GLORIA survey with completion of line 38. End full watchstanding activities.
12. 096/0020 Bridge now in control for transit to Honolulu. Gravity meter remained in operation to establish a land tie in Honolulu.

## Equipment Review: Comments and Operational Log for F3-and F4-88-HW

This review highlights the problems encountered, and resulting data gaps, with the various systems. Standard operational procedures are similar to those established for the 1986 surveys (Holmes et al., 1987; Normark et al., 1987) and are reviewed in Appendix I. A brief narrative summary of key events is provided for each system, generally in order from the most reliable system to most troublesome following the earlier F3 problems. The GLORIA operation is discussed separately. Complete reviews of the trouble-shooting and repairs required for each system are available in the technicians' logbooks.

**3.5-kHz High-Resolution Profiling System.** The 3.5-kHz reflection-profiling system operated smoothly from the beginning of the F3 leg. We slowed to stream the tow fish at 071/2020, and used the 3.5 kHz system immediately to continue the training of the temporary watchstanders. These early data, many of them taken before any other systems were operational, were logged as BA35-roll "0" in order to appease the data archive system. Fully official logging began with analog paper record (BA35-roll 1) at 072/0654. Although there were no operational difficulties, the record quality is marginal in areas of deep water (>4500 m) and the steep relief associated with the Molokai Fracture Zone. Because the IOS-maintained system does not have the option of using a longer pulse width (a casualty of the signal-correlation capability), we were unable to improve on the poor signal-to-noise ratio under the conditions noted above.

During leg F4, the system was shut down from 079/2127 to 080/0122 when the camera crew was transferred to a small boat alongside at about 0100. The tow fish, which is on the starboard side, had to be brought close to the hull for safety while the water taxi was standing along the FARNELLA (transfer was done at speeds of 2-3 knots with GLORIA still deployed, because of the problem with the launcher hydraulics). The tabulation below shows the periods of lost data during leg F4.

<u>Time Down</u>	<u>Time on line</u>	<u>Reason</u>
079/2127 080/0744	080/0122 080/0751	Secure during personnel transfer Paper feed stopped during two periods of 2 to 3 minutes. For the next half day, there were numerous episodes of a few sweeps lost but no more long intervals. Cause not identified.
080/1342 080/1519	080/1343 080/1702	Paper feed stops again. Three episodes of no paper feed. Total time loss is about 6 minutes.

**Magnetometer System.** The magnetometer was deployed after launching the GLORIA vehicle at approximately 072/0430. The system came on line with no difficulties, and we began officially logging data at 072/0646 (when the paper analog record was started). The magnetometer data are also recorded digitally on magnetic tape on the same recorder used for the gravimeter; this mag tape record begins earlier than the paper record because the gravimeter was already operational.

During leg F4, the winch motor on the magnetometer reel was not providing full torque and cannot pull the gear aboard at normal GLORIA tow speeds. Although operation was a bit slow, the magnetometer was retrieved with no adverse problems during the personnel transfer noted above. Loss of data was limited to the periods noted below.

<u>Time down</u>	<u>Time on line</u>	<u>Reason</u>
079/2127	080/0200	Retrieved while conducting personnel transfer for the film crew to water taxi.

**Expendable Bathythermograph System.** Expendable bathythermograph probes (XBT's) were deployed at least once each day to measure the thickness and temperature of the surface mixed layer and the temperature profile within the thermocline zone. Three types of probes were available: T-4 and T-6 probes are capable of profiles to 460 m and T-7 probes to 760 m; only the latter units can record the lower part of the thermocline zone. Because of a limited number of T-7 probes aboard the FARNELLA, we decided to deploy one T-7 each week and use the 460 m probes on the other days. The XBT system provided by NOAA handles recording, plotting, formatting (conversion of temperature vs depth data to inflection points), and transmission of the data.

Because the XBT system is not continuously in operation, the stations are recorded individually below. Unsuccessful, or partially successful stations generally result from breaking the wire to the probe or disruption of signal from the probe when the wire touches the ship's hull; in either case, a second XBT launch might be attempted. Positions for the stations are recorded in the data logs and shown in Figure 4. Where the record length is listed as "partial," the wire has probably come in contact with either the ship or one of the towed systems (air gun on starboard side or magnetometer on the port). Most of the failures during leg F4 were from gusting winds that blew the wire against the ship no matter which side was used for the launch. After the 7th partial record for leg F4 (on day 090), we constructed an extender for the launcher that would allow us to hold it closer to the sea surface. The next two launches in gusty wind conditions were definitely helped by this extender. On day 093, however, two launches (one from each side in cross winds) could not be saved even with the extender.

Under generally similar conditions of wind strengths and direction relative to the ship's bearing, our experience on leg F4 indicated that the port side has a higher probability for a successful launch of an XBT for two reasons: (1) The launch point is closer to the stern so there is less area of the side of the ship for the wire to be blown against, especially when using the extender; and (2) the tow cable to the magnetometer has a much flatter angle than the air-gun towing assembly, so the XBT wire has a better chance of sinking before coming in proximity with a towing cable.

<u>Station #</u>	<u>Day</u>	<u>XBT depth rating</u>	<u>Record length</u>
1	073	T-07 760 m	Full
2	074	T-06 460 m	Full
3	075	T-06 460 m	Full
4	076	T-04 460 m	Full
5	078	T-06 460 m	Full
6	079	T-06 460 m	Partial (130 m)
7	079	T-04 460 m	Partial (100 m)
8	081	T-07 760 m	Partial (342 m)
9	082	T-04 460 m	Partial (99 m)
10	084	T-04 460 m	Full
11	084	T-07 760 m	Partial (132 m)
12	084	T-07 760 m	Full
13	086	T-04 460 m	Full
14	087	T-04 460 m	Full
15	088	T-04 460 m	Partial (346 m)
16	089	T-04 460 m	Full

17	090	T-04 460 m	Partial (100 m)
18	091	T-04 460 m	Full
19	092	T-07 760 m	Full
20	093	T-04 460 m	Partial (103 m)
21	093	T-04 460 m	Partial (237 m)
22	094	T-06 460 m	Full
23	095	T-07 760 m	Full

**10-kHz Echo-Sounding System.** The 10-kHz bathymetric profiling system uses a towed vehicle similar to the one used for the 3.5-kHz reflection-profiling system. The tow fish was launched at 071/2020, but the system failed to operate. The problems were isolated to the tow vehicle component, and at 071/2235, the tow fish was recovered and the spare unit was deployed. The 10-kHz system remained inoperable, and the difficulties were again traced to the tow vehicle. Both vehicles were found to have problems in a junction box; one of the tow fish was repaired and relaunched at 072/0308. After several hours of practice in logging the data by the temporary watchstanders, the 10-kHz system officially came on line at 072/0654. From this point, the system worked well through the remainder of leg F3, and the only loss of record was during routine maintenance (changing blades and paper rolls). No problems on leg F4.

**Gravity Meter.** The gravity meter (LaCoste and Romberg, S-53) had been operational since the FARNELLA left Redwood City on 23 February. No problems were reported during the port call in Hilo, and a land tie was attempted using two gravimeters from the Hawaiian Volcano Observatory (HVO). After departure from Hilo, official logging of the gravity data began at 072/0455. The records appear normal until 072/0835, when the traces for total correction and cross coupling went off scale. The spring tension appeared to remain normal; the result was an apparent large vertical acceleration with a difference between the gravity reading and spring tension of about 80 mgal. The seas were rather calm at this time, so general sea-sickness was ruled out as a cause of the problem.

Inspection of the meter eventually located at least two problems, both of which could not be permanently fixed but whose effects could be minimized for the remainder of this leg. An intermittent in one of the cables and a dirty relay will have to be fixed in Honolulu.

A gravity meter from HVO provided a land tie in Honolulu as well. The land tie values are:

Honolulu harbor, Pier 40, JD 077	International gravity at meter: 10178.3
Honolulu harbor, Pier 40, JD 096	International gravity at meter: 10181.5

**Seismic reflection system.** The seismic-reflection system uses a 2,600 cm<sup>3</sup> (160 cu. in.) air-gun sound source and a two-channel streamer, whose total length including stabilizing drag line is about 800 m. The two active sections are 50 m long and are towed about 500 to 600 m behind the sound source. The signals are recorded on a MASSCOMP digitizing system, and one channel is displayed on a line scan recorder (LSR) with memory to produce an analog record.

The air gun is fired every 10 seconds and is recorded on both the MASSCOMP and LSR with a six-second record length. The memory capability of the LSR was used to print the field profile with a constant orientation (west ends of the profiles will be on the left side) and to reduce the vertical exaggeration of the profiles by printing each trace three times.

A series of problems plagued the seismic-reflection system for most of the leg. Although the streamer and air gun were deployed by about 072/0440, the logging did not begin until

072/0903. The reconfiguration of the recording systems since last year's operation resulted in serious interference between the 50 Hz (IOS) and 60 Hz (USGS) components. This problem was overcome with a temporary modification. Following the start of data recording, a series of annoying problems resulted in additional time lost with the system, as summarized below.

<u>Time down</u>	<u>Time on line</u>	<u>Reason</u>
072/0440	072/0903	Grounding problems in recording systems
073/1909	073/2236	Streamer noisy at speeds > 8 knots; had to add oil to all active and stretch sections.
075/0144	075/0228	Replace amplifier and filter systems owing to interference from the 3.5-kHz profiling system. This modification also removed the interference from the GLORIA system that has plagued the surveys since the original Hawaii operations.
075/2311	076/1548	Channel #1 became extremely noisy. The streamer was recovered and examined; some stretching had occurred, but not enough to account for the noise. Initial tests with instrumentation amplifier and storage scope show noise spikes being generated within the active section itself.

One other problem that affects the analog profile appeared during the last 36 hours of operation. The problem stems from the master air-gun trigger and deep-water delay systems. The deep-water delay box cyclically walks back and forth over a range of 10 msec as it locks on either the leading or trailing edge of its crystal clock. The result is an LSR single-channel record with stair-step offsets that obscure subtle angular relations between reflecting horizons.

In summary, F3-88-HW proved to be a test cruise for the many new and reconfigured parts of the air-gun reflection-profiling systems. The sediment cover appears relatively thin over much of the surveyed area, thus tending to minimize the impact of the lost data despite the fact that the system provided useable data for less than half of the cruise time.

During the Honolulu port stop, the problems in the deep-water delay box were fixed. The streamer was flaked on deck after launch of the 3.5-kHz and 10-kHz tow fish to check all connectors and look for other possible causes of the mechanical noise seen during the last day of operation during F3. The connectors were redone, but no other problems were identified. The air gun and streamer came on line at 078/0315 and the records were very clean with no undue noise. The following problems were encountered during leg F4:

<u>Time down</u>	<u>Time on line</u>	<u>Reason</u>
078/0834	078/0932	Leak in air hose near gun
079/2130	080/0140	Streamer only retrieved for personnel transfer to small boat coming alongside at 080/0100.
082/0059	082/0754	Masscomp crash after normal "control c" at end of previous tape. Analog record continued except for a few minutes while checking the trigger signal going to the Masscomp. System brought on line after trying new circuit boards, cables, etc without identifying the problem. The computer diagnostics gave no indication of any problem.
083/0757	083/0839	Masscomp goes off line again. Apparent cause was a stray keyboard input that the system did not understand. No physical repairs this time.

084/0002	084/0114	Scheduled gun change turned into repair of trigger line as well.
084/0558	084/0600	Replace belt in LSR; stylus alignment problem was affecting record clarity.
086/0137	086/0321	Tape recorder in Masscomp ceased operating; reason undetermined. Waited to start new tape until Larry had a chance to check the system and the start of a new line.
088/1850	088/2012	Scheduled air gun change but, as above, turned into a repair when the trigger line was found to be nearly severed. Cause not known for either case.
091/0431	091/0511	Gun firing became intermittent. Upon retrieving the gun, it was found that a piece of cargo netting had fouled the gun by crimping the air hose. The hose was not broken, but no other interference with gun operation was found. A new gun was installed during repairs, so the maintenance schedule now starts with new time zero.

**Shipboard Positioning Systems.** Most of the operational problems encountered during the first two GLORIA surveys off Hawaii resulted from limited position control for the tracklines (Holmes et al., 1987; Normark et al., 1987). The resulting sinusoidal tracks of questionable location have resulted in serious problems for processing the side-scan data. The position control during leg F3 is markedly improved over the 1986 surveys. The improvement can be directly related to three major changes: (1) The addition of rho-rho Loran C position determinations; (2) Improved usage and recording of available Global Positioning System (GPS) coverage; and (3) The addition of a real-time trackline display for the ship's bridge personnel that displays position relative to the desired survey line.

When the GPS constellation is available, the survey lines are generally within several hundred meters of the planned trackline. When the GPS satellites are not accessible, the preferred system is rho-rho Loran C. The study area on the northeast side of the Hawaiian Ridge is near or past the optimal range for the Loran C master station on Johnston Island, so there were several periods each day without optimum position control. During these periods, it was necessary to rely on transit satellite fixes and hyperbolic Loran C processed by the ABC system on the FARNELLA; a review of the serious limitations of this technique are fully discussed by Holmes et al. (1987) and Normark et al. (1987).

Early during line 001, which was the transit northeast to resume the F5-86-HW survey grid lines, the rho-rho Loran C position control was lost. At first, it was feared that all work in the eastern part of the EEZ northeast of the islands would suffer from poor navigation control. The system was modified, however, to lock onto a later phase of the Loran signal; this greatly improved the signal-to-noise ratio and by the end of the leg F3 operations, we generally had rho-rho position control during most of the intervals without GPS data. The extensive survey in the eastern part of the EEZ during leg F4 showed a marked improvement in position control relative to the F3 operations.

**GLORIA Side-Scan Sonar System.** The operation of the GLORIA system is covered in extensive logs by the IOS personnel, and a summary account only will be provided here. The pass record for the leg (note: one pass generally equals 6 hours of GLORIA data) and the number of files of GLORIA data are presented in Appendices 2 and 3.

Launch of the GLORIA vehicle for leg F3 commenced at 072/0413 and was completed by 0440. The system was fully operational by 072/0948 when logging began (i.e., start of pass

1). The system operated continuously, except for course changes, until survey activity stopped at 076/1521. No problems were encountered during the survey.

During recovery of the GLORIA vehicle, the hydraulic pump unit in the cradle/tow winch assembly was malfunctioning and caused a bit of delay in lifting the tow vehicle from the sea and securing it in the cradle. Repairs to the hydraulic pump and manifold system could not be completed in time for departure as scheduled for leg F4, but a temporary solution was tried that resulted in only a slight late delay of 2.5 hours. This attempted fix was not successful as was discovered during launch of the GLORIA vehicle during leg F4; the recovery of the vehicle at the end of F4 was done in the lee of Kauai and went very smoothly in the relatively calm waters.

**GLORIA shipboard image processing.** Cruises F3-88-HW and F4-88-HW saw an extension of the shipboard processing capability, following successful experiments on the IOSDL cruise *Charles Darwin 23* in May-June 1987. We have, in essence, introduced a shipboard 'shading' capability, performed optionally during replay on the GLORIA IBM PC (see Chavez, 1986 for a review of the standard processing techniques for the digital GLORIA data).

The purpose of this correction is to remove as much as possible of the range-dependent system response. As recorded, the GLORIA signal varies with range, over and above the variations resulting from the seabed geology. These variations arise from the directivity pattern of the GLORIA array, and the spreading and attenuation of sound in seawater. They are partially compensated by the applied time-varied-gain (TVG) function, but a significant variation in response remains. This is seen principally as a somewhat higher than average response at mid range, and correspondingly low response at near and far range; and particularly, a very low response in a narrow band on either side (but especially the port side) of the nadir.

In principle it should be possible to correct for this variation by determining appropriate values for the average response as a function of range, and modifying the recorded signal accordingly (by multiplying by the reciprocal of this function). In practice, this is harder than it sounds, because (a) all of the effects described above vary either directly or indirectly with water depth, so that ideally a whole family of correction functions would be needed; and (b) the perceived system response also depends on the backscattering coefficient, which is dependent on the angle of incidence of sound rays on the seafloor and is therefore also range dependent, in addition, of course, to varying as a function of seafloor lithology and microtopography.

In order to make a practical start, we restricted ourselves to attempting to correct only the sonographs obtained in deep water (greater than about 5000 m depth) well offshore from the islands, and applying a single correction function independent of lithology.

To estimate the system response, we compute the mean and maximum dn (digital number) values for each range element throughout a pass, using program AVSCAN (Figure 5). Over a smooth, sedimented bottom, and near the nadir, the mean profile seems to give the best result. However, where there are outcrops of strongly backscattering rock (e.g. basaltic seamounts), or where the maximum observable range is changing widely because of varying depth (and therefore causing large areas of acoustic shadow at far range), the envelope of the maximum values is more reliable. We take the reciprocals of the chosen values at each range, and 'normalize' them by multiplying by a constant factor: this is chosen so that the maximum corrected dn value (original times correction factor) is 255, the maximum that can be displayed in the replay system. It is only necessary to (1) determine a few values of the correction profile sufficient to define its overall shape; (2) then run program SHADMK, which will interpolate between them, and (3) build a file giving one correction factor for each range element. Finally, program SHADE is run; this takes a LASPSnnn.DAT data file (already corrected for slant range errors and anamorphic ratio by program GPROC), applies the shading

corrections, and writes the result to file LASHDnnn.DAT. The latter has exactly the same format as LASPS and can be written to the laser writer in the same way, using D2L.

Shading was applied in this way to all the deep-water data obtained to the northeast of Oahu and Molokai during leg F4, and the resulting sonographs were mosaicked on board. After some initial trials, we used the correction saved in file SHAD6 (see Table 1) from 080/0700 to 082/1759. We then introduced the slightly modified SHAD7 and used it from 082/1800 to 086/1159. However, it had been noticed that the raw (unshaded) data were showing rather low overall levels for the mean response and a systematic bias with the port side giving a lower response than the starboard side (see Figure 5, passes F3/1 and F3/2). The port gain was therefore adjusted at 0145/086 during pass 33 producing a more symmetrical overall response, as shown on pass F4/39 (Figure 5). Following this, we derived a new shading correction, SHAD9.DAT, which was used for the remainder of the leg.

TABLE 1: GLORIA shading corrections

Pixel number	SHAD6	SHAD7	SHAD9.DAT
2	1.20	1.11	1.14
100	1.11	1.11	1.08
200	0.88	0.88	0.95
300	0.75	0.75	0.82
350	0.71		0.78
390	0.75	0.80	
400			0.82
415	1.00	1.00	
425			0.92
435	1.20	1.20	
445			1.14
455			1.09
460	1.00	1.00	
470			0.74
480			0.62
497	0.52	0.52	0.62
500	0.75	0.70	0.70
520			1.00
530	1.00	1.00	
535			1.06
575	0.94	0.94	0.95
625			0.83
635	0.70	0.70	
650			0.80
670	0.64		
700	0.63	0.66	0.80
800	0.72	0.75	0.85
900	0.94	0.94	0.95
995	1.15	1.05	1.10

Values under 'SHADn' are the correction factors applied. Linear interpolation was used between given pixels. Pixel 2 is far-range port, 497 is near-range port, 500 is near-range starboard, and 995 is far-range starboard. Pixels 498 and 499 are always zero (to mark the ship's track).

The shading operation was quite successful, the greatest benefits being:

1. Enhancement of the signal near the nadir, particularly in the first sidelobe on the port side;
2. Enhancement of signal at far range;
3. Moderation of excessively high and variable returns in the nadir signal;
4. More uniform illumination across the majority of the scan;
5. Presentation of more realistic relative signal levels across the scan.

The main disadvantage is that the dynamic range of the corrected signal is effectively increased (correction factors range from about 0.5-0.6, to 1.1-1.2, giving a doubling of the original dynamic range). To encompass this in the printed data without overloading at the highest values, many data are written at a lower level (correction factor <1) than originally recorded, giving the prints a rather sombre appearance. This effect is enhanced by the fact that during replay to the laser writer, dn values are mapped to light intensities following a non-linear curve (the 'gamma curve'); if shading is to be applied routinely, it may be necessary to revise this curve.

The second 'disadvantage' is that the appropriate shading correction was found to depend strongly on lithology; the signal falls off more strongly with increasing range over smooth sediment (presumably as a function of increasing angle of incidence) than it does over lava (where backscattering may follow more of a corner-cube retro-reflector model, and not be strongly dependent on angle of incidence). 'Disadvantage' is put in quotes above, because this effect is actually providing additional geological information: comparing the backscattering level of the same area at different ranges could help to distinguish different lithologies. It does make production of a uniformly illuminated mosaic more difficult, however, and means that the shading correction must be chosen with great care and with sufficient regard for varying lithology. This will apply with equal force, of course, to shading applied during post-cruise processing too.

One final problem was the presence of biological interference. During the night the deep scattering layer was well developed, and showed up clearly in the near range on GLORIA (e.g., pass F3/1, Figure 5, where it partially fills the near-nadir minimum). If the shading correction was based only on daytime data (when the scattering layer is weak or absent, e.g., pass F3/2), the normally low signal at this range generated a high correction factor. When this correction was applied to nighttime passes, it amplified the scattering layer effect to an undesirable degree. If shading was based on nighttime data (with the layer present), then the short range response was unduly depressed for daytime applications. In practice we used a correction midway between the extremes, which gave a reasonable compromise; but this example illustrates the care with which shading corrections must be chosen.

## PRELIMINARY SUMMARY OF SCIENTIFIC RESULTS

These two GLORIA legs provided valuable information about several geological features near Hawaii. Especially prominent among these are the Molokai Fracture Zone, giant landslides from Oahu, Molokai and Kauai, and a large volcanic field on the Hawaiian Arch. Interesting results were also obtained concerning a large density-flow channel along the fracture zone, submerged reefs along windward coasts from Maui to Oahu, lesser landslides off windward Maui, the submarine east rift zone of the Wailau (East Molokai) Volcano, and young lava flows in the saddle between Oahu and Kauai.

**Molokai Fracture Zone.** The discussion below is based mostly on preliminary shipboard examination of the GLORIA data from F5-86-HW, and from the present F3-88-HW and F4-88-HW, together with the bathymetric and seismic reflection data from the latter two

cruises. The most striking finding is that the fracture zone consists of multiple strands or segments, and that part way along its length these segments branch and diverge, probably reflecting a change in spreading direction in this area during the Cretaceous (see also Atwater, 1989).

The GLORIA mosaics show that the Molokai Fracture Zone is characterized by a number of strong tectonic lineaments that strike ENE-WSW, along the presumed Cretaceous spreading direction. These lineaments occur in four separate bands 15 to 30 km wide, which will be referred to as bands A, B, C, and D, going from south to north (Figures 6 and 7). The overall width of the fracture zone ranges from 130 km at 154°W to 160 km at 152°W. Each band contains up to four individual lineaments separated by 5-12 km. Normal ridge-parallel spreading fabric is found between these bands, and almost everywhere strikes orthogonally to them, except in the immediate vicinity of the ENE-WSW lineaments where it curves in a sinistral sense towards them. The lineaments are composed of fault scarps or the colinear terminations of curved faults in the spreading fabric (Figure 6). Individual sections of lineaments range from 10 to 80 km long in band A to 150 km long in D, and are offset laterally from each other or are separated by short gaps of a few kilometers. With this reservation, single lineaments are continuous for up to 300 km.

This arrangement is remarkably similar to the style of present-day fast-slipping transform fault systems such as the Quebrada-Gofar at 3°-5°S on the East Pacific Rise (Searle, 1983). By analogy with the Quebrada-Gofar system, we take the ENE-WSW lineaments of the Molokai Fracture Zone to be fossil strike-slip transform fault traces, and suggest that each band of lineaments essentially represents an independent fracture zone. We infer from the sense of curvature of the spreading fabric that the ridge offsets were sinistral, so that a section across the fracture zone should encounter progressively younger seafloor going from south to north. This is confirmed by the variation in regional depth, which is 4900-5200 m in the south, 5000-5200 m between segments A and B, 4800-5200 m between C and D, and 4600-5000 m north of D. We covered insufficient area to estimate reliably the depth between B and C. A sinistral offset is also consistent with the offset of magnetic polarity boundaries across the Molokai Fracture Zone, which suggests an age contrast of about 15 Ma across the entire fracture zone (Atwater and Menard, 1970; Atwater, 1989). In the area north of the fracture zones in our survey, anomaly 34 (young end of the Cretaceous Quiet Zone) occurs at about 156.5° W, and anomaly 32 near 152°. South of the fracture zones, anomaly 34 is near 150.5° W; so the seafloor west of there is in the Cretaceous Quiet Zone (Atwater, 1989). From Atwater's (1989) maps, we estimate the average half-spreading rate from chron 32 to 34 was about 46 mm/a north of the fracture zone and 56 mm/a to the south. These estimates are not precise, however, because of evidence that ridge jumps occurred in this area during that interval.

Bathymetric profiles across the fracture zone, together with the nature of the GLORIA reflections, show that most of the ENE-WSW GLORIA lineaments are associated with north-facing scarps several hundreds of meters high (Figure 7). The one exception is at the intersection of bands B and D, where there are major ridges, as we discuss below. The relief on the fracture zone scarps increases from 400-500 m (plus 0.4-0.6 s two-way time equivalent buried beneath sediments) at fracture zone A, through 700 m (+0.3 s) at B and C, to 1200 and 1600 m (+0.2 to 0.4 s) at D. To the south of these scarps, the seafloor falls away in gentle dip slopes that expose basement along the lineated spreading fabric near their crests but become progressively buried by sediment as they descend into the next fracture zone valley south. Draped sediment thickness is in the range 0.0-0.2 s on the dip slopes, and ponded sediments reach 0.6 s thick in the valleys, where the sediment surface usually slopes gently to the south or east.

The north-facing scarps imaged by GLORIA are thought to be the fossilized traces of once actively slipping transform faults. At presently active transforms, exactly analogous fossil

traces are colinear with the active transform fault traces. As found on other fracture zones (Searle, 1986; Tamsett and Searle, 1988), these scarps preferentially face the younger seafloor. The reason is not entirely understood, but is probably a localized effect caused by the end of a spreading segment in contact with a fracture zone wall being depressed, due to hydrostatic head loss, below its normal equilibrium depth. This creates a vertical step, up from the end of the spreading center onto the older crust, that gets frozen into the inactive fracture zone limb as a scarp facing the younger crust. It is in the opposite sense from the major topographic step predicted by Menard and Atwater (1969) on the basis of the age offset across a fracture zone (deeper seafloor predicted on the older side). We also see this latter effect across the Molokai Fracture Zone, but it occurs on a broader scale via the relatively gentle south-dipping slopes of the fracture zone ridges, and is quite separate from the smaller-scale scarps that show up as tectonic traces on GLORIA data (Figure 7).

Perhaps the most remarkable feature of the Molokai Fracture Zone is the fact that the trend of segments C and D ( $076^{\circ}$ ) is about  $10.5^{\circ}$  different from that of segments A and B ( $087^{\circ}$ ), and that, in the easternmost part of our survey area, the two sets of fracture zone traces therefore diverge eastwards. Segment C lies 30 km south of D, and merges with B at  $153\text{-}154^{\circ}\text{W}$ . Similarly, D and B converge westwards to meet at  $155^{\circ}\text{W}$ . We interpret this to mean that during the Cretaceous there was a double fracture zone here, of which traces A and B are the fossil remains of one period, and C and D are those of another, separated by a  $10^{\circ}$  change of spreading direction. Thus two fracture zones (A and D) are inferred to be buried beneath the Hawaiian Ridge to the west of  $155^{\circ}\text{W}$ . Interestingly, the spreading fabric remains everywhere orthogonal to the fracture zone traces: south of A and B it strikes  $173\text{-}176^{\circ}$ , while north of C and D it strikes  $165\text{-}168^{\circ}$ . West of the Hawaiian Ridge, the Molokai was shown on available bathymetric charts as a single fracture zone trending  $076^{\circ}$ . Because we did not know the true curvature of the traces, however, it was not clear during the cruise whether this trend is more continuous with strand A or D and therefore whether A or D is the older. Post-cruise study has, however, resolved this (Figure 8).

Reference to the Seasat-derived gravity field (Haxby, 1987) shows that the traces of the major fracture zones Mendocino, Pioneer, Murray, and probably also Molokai and Clarion, were concave south during most of the Cretaceous Quiet Zone, striking ENE in the earlier part and curving to nearly due east at the end. This is confirmed by studies of the regional bathymetry (Sager and Pringle, 1987) and magnetic anomalies (Atwater, 1989). Rea (1970), together with these more recent studies, suggests that there was a counter-clockwise change in spreading direction, from E-W to ENE-WSW, near or shortly after chron 34. GLORIA survey cruises F5-88-HW and F10-88-HW imaged two fracture zone traces, with a N-S separation of about 100 km, west of the Hawaiian Ridge (Figure 12; Torresan et al., 1989; MacGregor et al., 1989). For the present, we shall call the southern trace E and the northern one F (Figure 8). E strikes about  $075^{\circ}$ , and F about  $79^{\circ}$ . We believe they continue under the Hawaiian Ridge, each changing direction about  $10^{\circ}$ , to join traces A and B east of the Ridge (A being continuous with E, and B with F, Figure 8).

MacGregor and others (1989) have suggested that trace F, which was unknown before their cruise, be called the Kauai Fracture Zone to distinguish it from the Molokai (trace E). But if we are right in believing B and F to be the same fracture zone, then it is this northern trace that underlies Molokai Island and should be named Molokai Fracture Zone. We would prefer to see the southern trace (A-E) named Maui Fracture Zone, since it passes beneath the south coast of that island. Such nomenclature could, however, lead to confusion (A, B and E have all been considered parts of the Molokai Fracture Zone in the past), so a more practical (but also more prosaic and somewhat less accurate) scheme would be to call A-E the South Molokai Fracture Zone and B-F the North Molokai Fracture Zone.

Traces C and D then represent the younger spreading direction, following the counter-clockwise change near chron 34. Because the two Molokai fracture zones both had sinistral offsets (Figure 9A), a counterclockwise change in spreading direction would have caused both to become leaky, opening up rhomboid-shaped gaps (Menard and Atwater, 1968; Figure 9B). As spreading continued along the new direction, new spreading centers would have become established within the enlarging rhomboids. Initially these would probably have consisted of several closely spaced transform faults separated by extensional relay zones or short spreading segments (Figure 9C), although eventually it is likely that some of the segments and transforms would be eliminated by rearrangement of the plate boundary, probably via ridge propagation, leaving two transforms at the margins of each rhomboid containing one or more intervening spreading segments (Figure 9D). It is unlikely that original (pre-change) spreading segments would propagate across the rhombuses, because their opposite flanks would consist of old, strong lithosphere from the far side of the fracture zone.

If this interpretation is correct, the Molokai Fracture Zone just east of Hawaii may represent one of the best surveyed examples of the effect of changing spreading direction on the tectonic pattern and morphology of a fracture zone. It may be relevant that the fracture zone relief is greatest near the site of the change (junction of B with D): the soundings along our survey lines show minimum depths of around 3900 m there, but published charts (Chase et al., 1970, 1981; Wilde et al., 1980) suggest that the seafloor shoals to 3400-3600 m between 153.3° and 154°W on strand D, and to about 3100 m at the junction of B and D near 21.7°N, 154.5°W. In the latter position, the nature of the fossil transform trace also seems to change, from a north-facing scarp to a line of more symmetric whale-backed ridges (loci of the shallowest water depths). We speculate that these ridges may reflect intrusions or diapirs formed in response to the new N-S tensional stress associated with the early stages of the change of spreading direction.

**Relationship of the fracture zone to Hawaiian volcanism.** The present morphologic expression of the fracture zone diminishes to the west, and the seafloor expression of the tectonic lineaments becomes less continuous as they are buried under the sediments of the Hawaiian Trough. Fracture zone A, however, can be traced directly to an area north of Hawaii and east of Maui, where its lineaments appear to extend beneath the Haleakala Ridge. A few ENE-WSW lineaments a short distance northeast of Maui may be associated with fracture zone B, but their identification is much less certain.

Fracture zone A, extended westward, is adjacent to a discontinuity in the Hawaiian Ridge, a discontinuity represented by a gap in volcanism between Haleakala and Kohala. This gap is expressed in various ways. Spatially, there is an anomalously long 100 km gap between the summits of Haleakala and Kohala (Figure 10), whereas the gaps between most Hawaiian volcanoes are generally about 50 km. A correspondingly large temporal gap is estimated from differences in shelf-break depth for the two volcanoes. The Haleakala shelf break is now at a depth of 2000 m and the Kohala shelf break is at a depth of 920 m; if the average rate of subsidence has been 2.5 mm/yr, the depth difference corresponds to an age difference of 170 ka (Moore, 1987; Moore and Campbell, 1987). Finally, there is a topographic gap corresponding to the Alenuihaha Channel that is 1800 m deep (much greater than the depth of passes between other islands of the chain northwest of Maui).

Corresponding to the gap between Haleakala and Kohala is the anomalously large volume and long and complex history of Haleakala. The gap between the volcanoes does not represent an interruption in output from the Hawaiian hotspot but merely reflects the prolonged duration of the growth of Haleakala.

We suspect that the Molokai Fracture Zone was responsible for the enhanced growth of Haleakala and corresponding gap between Haleakala and Kohala. The fracture zone could have

effected this in various ways. For example, the thicker lithosphere on the south (older) side of the fracture zone might have retarded ascent of new magma, which would have had a shorter ascent to the north. The fracture zone itself may have provided an easier lateral path for magma to follow, promoting the eastward extension of the Haleakala Ridge instead of building a new edifice. And the north-facing faults of the fracture zone may have stabilized the toe of Haleakala's otherwise unbuttressed south flank, thereby impeding landsliding that might have opened new passageways for magma to ascend through the southern flank of the volcano.

Similar effects along strand B of the fracture zone may have similarly enhanced the growth of the long eastern rift zone of the East Molokai volcano (Wailau) and of Penguin Bank and retarded development of the Lanai and West Maui volcanoes.

**Hawaiian Arch volcanic field.** A surprising result of this survey was discovery of a large volcanic field on the Hawaiian Arch (Figure 11). The existence of this field was not a total surprise because we had been primed for it by GLORIA's 1986 discovery of a smaller volcanic field on the Arch southwest of Hawaii (Normark et al., 1987) and by still earlier indications of Cenozoic volcanism on the Arch near the Mohole-site survey area (Spiess et al., 1969; Wallin, 1982). We were not prepared, however, for the size and complexity of the volcanic field; we can give here only a cursory account of this volcanic field because most of its western margin lies west of the survey area for leg F4.

In size, this lava field is to the lava field found in 1986 southwest of Hawaii as something like Texas is to Rhode Island. Like that other field, this one can be divided into a younger part having little sediment cover and an older part clearly mantled by sediment. Most of the younger part is a contiguous belt that occurs along the west edge of our survey area and extends farther west. The fraction that we mapped stretches down both the northern and southern flanks of the Hawaiian Arch for a total distance of about 300 km and covers an area of about 15,000 km<sup>2</sup> (compared with an area of ~10,000 km<sup>2</sup> for the Hawaiian Islands) to an average depth of at least 10 m and perhaps more than 30 m, for a total volume of several hundred km<sup>3</sup>. All of this lava cover (of the younger part of the field) seems to be of similar age; except for a few minor cases, we have found no significant backscatter contrasts of the sort used by Holcomb et al. (1988) to differentiate age groups among the large flows from the Puna Ridge. Some separate flows farther east, grouped with the larger western flow field on Figure 11, do appear to have slightly lower backscatter and presumably greater age. With its many separate tendrils extending down the southern flank of the Arch, the southern part of the young lava field looks on our mosaic like a giant dragonfly swooping down onto Oahu.

The older part of the volcanic field covers another 15,000 km<sup>2</sup> east of the younger flow field, and old vents protruding through the younger field suggest that the older material might also underly much of the younger field. In most places, the older material is thick enough to conceal the abyssal-hill topography, which generally has a relief of 100-200 m (but could be less here on the flank of the Hawaiian Trough as a result of volcanoclastic fill from the islands). The total volume of the volcanic field must therefore be at least several thousand km<sup>3</sup>.

Flows of several different ages can be distinguished in the older part of the volcanic field. Whereas distal lobes of the large western flow appear to overlap the toe of the giant landslide from Oahu, the toe of the landslide appears to overlie another mappable lava flow about 70 km farther east. Because that overlapped lava flow is clearly younger than other volcanic fields nearby, the volcanic field must have been active long before the landslide occurred.

Although GLORIA cannot resolve many morphologic details on the lava flows, the images do seem to show lava channels in a few places. The 3.5 kHz profiles suggest that many of the lava flows have thick inflated interior plateaus surrounded by haloes of thinner, uninflated lava.

Irregularly shaped patches of anomalous backscatter suggest that some parts of the flows have different surface roughness. It seems likely, therefore, that a variety of morphologic flow types occur, and that some of the eruptions have been sustained for long intervals. Another possibility is that a part of the very large young flow field consists of rapidly extruded 'flood basalt'.

Several tens or hundreds of eruptive vent structures occur within the volcanic field, and several of the younger lava flows can be traced to specific vent areas. The vents vary greatly in morphology and possibly also in chemical composition. Included are cones (ranging in size from barely resolvable to a few large seamounts thousands of meters high), cratered cones, crater rows, and various irregularly shaped edifices. Especially distinctive are numerous convex dome-like structures that resemble subaerial domes of trachyte or rhyolite (see also Spiess et al., 1969).

The most striking edifices assumed to be built by vents are large volcanic ridges and linear chains of smaller vents. We imaged at least five distinct ridges, whose western ends are shown as black bands on Figure 11. These ridges have lengths that vary from 80 km to more than 180 km, and separations (perpendicular to their lengths) of 30 km to 100 km. The most linear segments are generally narrow (5-10 km wide), a few hundred meters high (average about 600 m), and sharp crested, with strikes between  $069^{\circ}$  and  $089^{\circ}$  (subparallel to either the late Cretaceous or early Paleogene Molokai Fracture Zone trends). The 3.5 kHz profiles suggest that these ridges are capped by sediment at least a few decameters thick, and the airgun records probably indicate a few tens of meters of sediment on some of the less steep summits. At their western ends these ridges either terminate fairly abruptly or break up into lines and clusters of central vents, which are mostly truncated cones up to 8 km in diameter. The central vents appear to have relatively thin sediment cover and therefore may be much younger than the continuous ridges. The chains and clusters of central vents commonly follow curvilinear trends that gradually veer westward to strikes of  $097^{\circ}$  to  $102^{\circ}$  and may be approaching the trend of the Hawaiian Ridge. Along the ridges and vent chains in a few places are large, roughly circular seamounts up to about 2000 m high and 20 km in diameter. In addition to the linear chains, many individual or small clusters of volcanoes appear to be scattered randomly over the western part of the volcanic field.

The continuous volcanic ridges are of particular interest. They do not appear to be associated with linear valleys or changes in regional depth of the seafloor or basement. They have small, symmetric free-air gravity anomalies generally of about +10 to +20 mgal, but as much as +60 mgal over the largest edifices; in the latter cases, the lithosphere appears to be slightly downward warped on either side of the ridge. The ridges have small magnetic anomalies of about -70 to -220 nT, either roughly symmetric or negative to the northwest; this is consistent with their being normally magnetized, but whether the anomalies result entirely from topographic effects will have to await detailed modelling. We see no change in the nature or trend of the surrounding tectonic spreading fabric in the vicinity of the ridges, and in particular no curving such as is commonly associated with the nearby fracture zones (although it is perhaps possible that such effects might be buried under the volcanic edifices). Several of the ridges appear to have significant caps of sediment, and rocks dredged from them (Clague et al., 1989) appear old, with strong weathering and thick manganese crusts. The ridges are morphologically similar to many of the Musicians Seamounts (Rea and Naugler, 1970), which also have strong ENE-WSW linear trends and are dated Late Cretaceous to early Paleogene (Clague and Dalrymple, 1975; Sager and Pringle, 1987).

The absence of curved spreading fabric, of linear valleys, and of depth offsets, together with the close N-S spacing between adjacent ridges and their singular morphology, all suggest that these ridges are not simple fracture zone traces, although where they are narrowest and most linear they closely follow one of the observed Molokai Fracture Zone directions. Further careful

examination and modelling of the potential field data across these ridges is necessary to check this conclusion.

In many respects, the ridges show a remarkable similarity to the en echelon 'cross-grain ridges' recently described in the area east of the Line Islands by Winterer and Sandwell (1987). In particular, those authors found that similar ridges in the equatorial Pacific tend to have a razor-back morphology where they follow fracture zone directions but consist of lines of cones elsewhere. Winterer and Sandwell (1987) believe that the ridges reflect tensional cracks in the lithosphere, and we think a similar origin is likely in this area, though the source of tension may not necessarily be the same as they propose (i.e. lithospheric boudinage). One possibility is that there were many short-offset fracture zones in this region in the late Cretaceous: Atwater (1989) shows, somewhat schematically, several small sinistral offsets in the western side of anomaly 33 between the Molokai and Murray fracture zones. Such fracture zones would have been placed into tension by the late Cretaceous spreading direction change, offering routes for magma to reach the seafloor and build volcanic ridges.

A similar explanation, however, cannot apply to the Musicians Seamounts, many of which look morphologically similar to our volcanic ridges but which extend north of the Murray Fracture Zone into a region of probable dextral fracture zone offsets. It also fails to explain why similar ridges were not built on the Molokai Fracture Zone itself. Perhaps there was a regional source of magma (a hot spot?) in this region in the late Cretaceous, as suggested by Sager and Pringle (1987) that did not extend as far south as the Molokai Fracture Zone. Magma from such a hotspot might have leaked along all fracture zones above it, if they were in tension from some other cause, such as ridge-parallel thermal contraction (Turcotte, 1974; Turcotte and Oxburgh, 1973).

An important source for the large younger part of the lava field is a particular volcanic ridge trending east-west near 24° 00'N, 157° 15'W, a part of one of the major volcanic lines described above. Lava flows appear to emanate from several points along a cluster of large domes along this ridge. Another major source probably occurs on the next ridge to the north, where a large seamount occurs near 25° 00'N, 157° 10'W. We see evidence on GLORIA of other young, but smaller lava flows arising from vents farther east along both of these ridges: a moderate-sized field seems to have flowed from the 24° N ridge near 156° 40'W, and a small field (a few individual flows) has come from the 25° N ridge near 156° 50'W. These flows are all relatively recent; 3.5 kHz profiles show them to be covered by less than 2 m of sediment, i.e. below resolution of the system. We do not know the ages of the linear ridges themselves, but suspect they may be somewhat older; certainly their more easterly portions do not show evidence of very recent, extensive lava flows on GLORIA sonographs, and 3.5 kHz profiles over these areas show normal pelagic sediment drape, not buried lava flows. However, we cannot say at present whether this implies a relatively recent but pre-Hawaiian (pre-Pleistocene?) age for the ridges, a Cretaceous age, or something in between. Their similarity, however, to some of the linear ridges in the Musicians Seamount Province (Rea and Naugler, 1970) suggests that the two sets of features may be closely related, and we note that the Musicians Seamounts are probably Late Cretaceous to Early Paleocene in age (Clague and Dalrymple, 1975). The ridges that apparently vented the oldest lava flows have slightly different trends, more westerly or WNW, than other ridges near them; it is therefore possible that ridges of different ages have recorded changes in the local stress field.

Other linear ridges with similar trends can be seen on the 1:2,000,000 scale regional bathymetry north of the Hawaiian chain, extending in a band from our survey area to, and possibly including, the Musicians Seamounts (Figure 12). This band of ENE-trending ridges has its southwestern boundary on the south limb of the northeastern Hawaiian Arch, some 200 km NNE of the island chain. From there it extends from 200 km to perhaps as much as 600 km to the ENE, and apparently terminates north of the Arch roughly along the 5000 m isobath. A

similar band of ridges is not obvious on the southwestern arm of the Hawaiian Arch or the segment southeast of Hawaii. This restricted geographic extent of the ridges suggests that: 1) the ridges are associated with the Arch but have developed on only one side because of some asymmetry; or 2) that they formed independently of the Arch, perhaps being restricted to seafloor of a given age (possibly associated with the Cretaceous change of spreading direction discussed under the Molokai Fracture Zone section of this report?); or 3) they are associated with the Arch but formed only where some pre-existing lines of weakness predisposed the lithosphere to fracture.

It would appear that the ridges are acting as weak lines, and are being opened or reopened, possibly in response to flexing of the lithosphere at the Hawaiian Arch. We do not yet understand why they tend to follow Cretaceous fracture zone trends or why they appear to be restricted to the Arch north of the islands, but we are considering various possibilities. The apparent ease with which the ridges can supply large volumes of lava over fairly short intervals may indicate that a magma plume feeding the Hawaiian shields also extends several hundreds of kilometers from the islands. If so, the plume would have a diameter similar to those inferred for the early Tertiary North Atlantic (Iceland) and Canary Islands plumes (e.g. White et al., 1987).

**Sinuuous channel in the Molokai Fracture Zone.** An unexpected feature encountered shortly after the commencement of F3-88-HW is a peculiar channel along the central part (strand B near its junction with strand C; Figure 8) of the Molokai Fracture Zone, slightly east of the Hawaiian Arch axis and just a few kilometers beyond the end of the last F5-86-HW survey line. The well-imaged part of the feature is about 30 km long and 1.5 km wide (Figure 13). It resembles a lunar sinuous rille, having a flat floor, nearly constant width, straight segments interspersed with smoothly curved reaches, and cusps along the inner edges of the sharper curves. Less sharply imaged extensions of the channel, having similar width but defined only by diffusely bright edges with no relief resolved, can be traced in both directions for a total length of more than 100 km (Figure 14).

The western half of the channel runs along the southern edge of a principal valley of the fracture zone (between strands B and D) at a depth greater than 5000 m; but in the vicinity of its well-imaged segment near 153° west longitude it crosses the structural grain obliquely and appears to continue into a parallel, slightly deeper, narrow valley of strand B about 20 km to the south. Sub-bottom profiles (Figure 15) reveal a contrast between the channel-like feature and surrounding sediments, which are well-bedded and more transparent. The GLORIA images also show that the backscatter from the channel is stronger than from its surroundings and probably has coarser material on or just below its floor. The profiles show that the channel slopes down from west to east, with a nearly constant gradient of about 2.4 m/km over three segments between profiles 1, 2, 5, and 6 (Figure 16). (This constant gradient along the channel contrasts with gradients along two other paths that the channel might have followed but apparently did not. The gradient between profiles 3 and 4, farther east along a blind branch of the main northern valley, is only about 0.2 m/km. In addition, the coarse-surfaced channel in the branch valley seems narrow on profile 3 and may be entirely absent on profile 4, as if it never entered that branch or died out shortly after doing so. A middle valley also possesses a narrow channel-like band of coarse material, shown by a dashed line on Figure 14, but this valley also is blind and has a steeper variable gradient, shown by line segments 2-7-8 on Figure 16.)

The transverse profile of the channel is not well determined. Along most of its length, the well-imaged segment looks like a channel at least several meters to tens of meters deep; in both images (Figure 13) the near edge is dark, like a wall facing away from GLORIA, and the far edge is light, like a wall facing toward GLORIA. Along one 5-km stretch (R of Figure 14), however, the southwest edge appears bright in both images, under opposite look directions, like a narrow levee-like ridge instead of a northeast-facing wall. And on pass 2, the image the northeast wall

of the same stretch also appears to have a very narrow bordering shadow, as if it too might be a low levee. Alternatively, the marginal brightening may be a result merely of coarser material deposited along the edge of a density flow. Similar grain-size effects are known to occur on large debris-flow deposits, such as the Alika slide described by Lipman et al. (1988). Similar channel-like features observed by GLORIA elsewhere, such as the extensive braided stream patterns in the Bering Sea, have been shown to lack relief (Karl et al., 1987), and the backscatter pattern seen across this channel might simply reflect grain-size variation instead of relief. This channel, in fact, exhibits no relief where our 3.5 kHz reflection profiles cross it.

Nevertheless it seems clear, from the two different passes with opposing look directions, that much of the well-imaged segment is a true channel having negative relief. We suggest that in most of its reaches the channel-like feature is merely a deposit of coarse material deposited by a density flow, that this flow incised a channel where it crossed sediment draping slightly higher ground between graben structures, and that it built marginal levees where it adjusted from erosional to depositional regime along the stretch just downstream from the incision. Duration of flow was long enough in the incised segment for lateral cutting to produce cusps on the inside banks of bends.

This feature is similar in several respects to the Cascadia Channel (EEZ Scan 84 Scientific Staff, 1986), which is thought to have meandered through several parallel valleys of the Blanco Fracture Zone. This channel also resembles to a lesser extent some other deep-ocean channels imaged by GLORIA, such as those on the Amazon and Mississippi fans (Damuth et al., 1983; Flood and Damuth, 1987; Kastens and Shor, 1985, 1986). This channel within the Molokai Fracture Zone, however, is much smaller in all dimensions than the sinuous channels of the fans noted above.

Despite its similarities to submarine channels elsewhere, this example seems unique in its isolation from a major landmass or continental shelf. Presumably, such channels are produced by density flows from extensive high-standing source areas, and such sources are scarce in the central Pacific. For this channel, only two sources seem possible; one is relatively distant on the Hawaiian Ridge and the other is nearby on the Hawaiian Arch.

The Hawaiian Ridge is 200-300 km to the west. It is attractive as a source because its many large landslides could produce material for density flows, and the channel could follow fracture-zone valleys that remain near depths of 5000 m all across the Hawaiian Arch. A problem with this explanation is the Hawaiian Trough, which separates the Ridge from the Arch with a minimum depth of 5400 m. A modern-day density flow from the Hawaiian Ridge would have to climb at least 400 m up the east flank of the Trough in order to reach the deepest valleys across the Hawaiian Arch. Although the large landslides from Oahu and Molokai probably climbed high enough onto the Arch to feed such density flows (large blocks from these slides presently lie as much as 300 m above the floor of the trough), those landslides seem to lie too far north to have fed this channel. The GLORIA images show that other landslides have moved eastward off the flank of the Haleakala Ridge, but those examples are much smaller, less chaotic, and probably moved much more slowly; we doubt that they could have fed material to the channel.

Some of these objections might be overcome if the channel predated subsidence of the Hawaiian Trough, which in this vicinity would have occurred at about 1-2 Ma. Since then only a few meters of acoustically transparent pelagic sediment would be expected to accumulate, and it is known (e.g., Clague et al., 1988) that GLORIA readily penetrates such thin veneers to reveal structure beneath. It seems reasonable, therefore, that the channel could predate the present Trough; if so, it could have been fed by a landslide moving southeastward from Molokai. At least one such landslide is thought to have occurred from the southeast flank of the West Molokai Volcano before the growth of East Molokai Volcano. This alternative still does not completely eliminate the problem of the Trough; the Hawaiian Ridge should have always been surrounded by

a trough of subsidence, no matter where it was in the past, and any density flows from the Ridge would have to climb out of that trough in order to reach the fracture zone. A developing segment of the Trough in front of the Ridge, however, should have been shallower and might have been easier to cross than a more deeply subsided segment alongside the island chain.

A possible local source for the channel is about 15 km northwest of profile line 1 (Figure 14), where an especially high ridge reaches the greatest elevation (depth less than 3600 m) seen along the imaged segment of the fracture zone. Although the southeast flank of this eminence is the dip slope of a fault block, its surface appears especially rugged on the GLORIA images, as if its blanket of sediment had been shed. The surface of this possible landslip scar rises more than 1400 m over a distance of 12 km from the floor of the valley, a gradient of about 110 m/km. This "scar" has an area of about 200 km<sup>2</sup>; if it shed a layer of sediment 20 m thick (somewhat less than thicknesses typical on Figure 15), the volume of the landslip would be about 4 km<sup>3</sup>. A deposit having an equal volume, thickness of 10 m, and width of 2 km would require a length of 200 km; a thicker or wider deposit could be shorter. These values seem to accord roughly with the observed width and length of the channel; the hypothesized source area seems capable of supplying the needed volume of material.

The chief uncertainties with the hypothesis for a local source are the nature of the triggering event and stability of sediment in the source region (for possible seismic triggering, see Kastens, 1984), the number of flow events involved, the flow mechanism (debris flow or turbidity current), and the uncertain ability of such flows to incise a channel. These questions strike us as intriguing subjects for theoretical consideration. Another point against the hypothesis for a local source is that on some GLORIA images the channel appears to extend farther west than the hypothesized source area. A point in favor of this hypothesis, however, is the likelihood of repeated earthquakes in this area during the last few million years as the Molokai Fracture Zone was flexed by development of the Hawaiian Arch.

**East rift zone of East Molokai (Wailau) Volcano.** A prominent bathymetric ridge about 60 km NNE of Maui has long intrigued Hawaiian geologists as a possible submarine rift zone, and we were eager to see what it would look like on the GLORIA imagery. It does, in fact, look very much like a submarine volcanic ridge similar to the Puna (Kilauea) and Hilo (Mauna Kea) ridges east of Hawaii, possessing the characteristic hummocky topography and lacking signs of large-scale slumping. Because this ridge trends east-west with no sign of turning south toward the West Maui volcano, we infer that it is a submarine east rift zone of the East Molokai (Wailau) volcano. If that is correct, the East Molokai rift zone was about 120 km long, similar to Kilauea's east rift zone but shorter than the Haleakala Ridge.

We had hoped to make a detailed comparison between this submarine ridge and the Puna and Hilo ridges. The latter two ridges differ from each other in a way suggesting to some observers that small-scale landsliding produces a characteristic 'fish-scale' topography consisting of many short terraces enhancing the hummocky appearance of older (Hilo, age about 130 ka) ridges compared with younger (Puna, still growing) ones. Unfortunately, the images of the East Molokai ridge are rather blurry, and it may not be possible to make a reliable comparison. It appears, however, that the East Molokai ridge (age about 1.5 Ma) is similar to the Hilo ridge. Much older Cretaceous seamounts also have terracettes differing little from those of the Hilo and East Molokai ridges. This suggests to us that whatever process produces the terracettes must occur mostly during the few hundred thousand years after a ridge stops growing. We do not see why landsliding should behave in such a manner; therefore we suspect that some other process is responsible. We suggest that the terracettes arise from volcanoclastic sedimentation, such that primary lava-flow hummocks accumulate flat-surfaced caps of sediment that reach limiting thicknesses within a few hundred thousand years. Later sediment cannot accumulate because low cohesive strength leads to mass failure after the limit is reached. According to this hypothesis,

the terraces cannot grow further unless lithification increases the yield strength of the material.

**Wailau and Nuuanu Landslides.** Moore (1964) first proposed that the irregular, large topographic features interrupting the Hawaiian Trough northeast of Oahu and Molokai were landslides from the flank of the two Hawaiian islands. Although this suggestion did not prove popular when it was proposed (Langford and Brill, 1972), there is strong evidence that the northern half of the Wailau volcano on eastern Molokai is missing--as was suggested by the first geologists to study Hawaii (e.g., Dana, 1849). Holcomb (1976, 1985) presented stratigraphic evidence showing that half of the volcano and its caldera were missing, and he specifically proposed that a large landslide was the most likely explanation, estimating the missing volume of Wailau at 500 km<sup>3</sup>.

In addition, evidence has been steadily accumulating for large-scale mass wasting of submarine slopes along several Hawaiian volcanoes. U.S.G.S. cruises in 1976 and 1978 not only surveyed the slides north of Oahu and Molokai but also documented the existence of the Alike slide on the west flank of Mauna Loa volcano on Hawaii (Normark et al., 1979). Moore and Moore (1984) presented evidence that a giant wave swept across much of Lanai, and they proposed a landslide as the cause. The initial GLORIA survey of the southwestern side of the Hawaiian Ridge clearly documented both the Alike slide (of at least 1000 km<sup>3</sup>) and a feature of similar size southwest of Lanai (Lipman et al., 1988). A major expectation of the leg F4 survey was to document the extent of the large landslides east and north of Oahu and Molokai that we herein term the Nuuanu and Wailau landslides after the Nuuanu Pali (inferred headwall of the Oahu slide) and the original name for the East Molokai volcano, respectively.

The GLORIA images and associated seismic-reflection profiles (Figures 17 and 18) show that the combined Wailau and Nuuanu slide deposits extend well past the area of large topographic features in the Hawaiian Trough that drew Moore's (1964) attention initially. Figure 19 shows the distribution of slide blocks as recorded on the GLORIA images, and Figure 20 is a summary of the major characters for the Wailau and Nuuanu slides and several other mass-wastage deposits. The area over which we recognize slide debris (not implying a complete cover of debris) is about 17,000 km<sup>2</sup>. This estimate is based on the recognition of high backscatter from discrete sea-floor objects, which must be at least 50 m wide to show up on GLORIA images. The area estimate was checked against both the air-gun and 3.5-kHz profiles that show both positive and negative relief features of the appropriate scale to conform to the major (those more than half a kilometer wide and tens of meters high) GLORIA targets, and the same limits were observed. For the Wailau slide, debris has moved as much as 190 km from the break in slope at about 1200 m water depth; this is nearly 210 km from the intact caldera segment on the volcano. For the Nuuanu source, the corresponding distances are 215 km and 235 km, respectively. At this point, we cannot distinguish the particular debris components of the two volcano sources (see below). For both volcanoes, the maximum fall height is on the order of 6 km or slightly more.

The volume of the deposit is more difficult to assess. Unlike slides and debris flows from sedimented continental margins, where the mass-wasted material tends to completely cover the sea floor in the depositional area, we have only recognized discrete blocks. We estimated the volume for separate size-classes of the debris: blocks having long dimensions >20 km, 15 to 20 km, 5 to 15 km, and <5 km. This yields a volume of 2300 km<sup>3</sup>, about twice that of the Alike slide (Lipman et al., 1988). If half of the total came from each volcano, then the amount from Wailau is about twice that originally estimated by Holcomb (1985). The two largest blocks, one from each volcano, account for nearly 80% of the total volume.

The most convincing evidence for the slide origin of the "bright spots" on the GLORIA image is their distribution, fanning and decreasing population density away from the large segments at

the base of the ridge (Figure 19). These kinds of backscatter targets are generally uncommon elsewhere within the study area, and they match closely the images from the Alike and Lanai slide deposits. Using the surface ship 3.5-kHz profiles, we could not distinguish block shapes because of the great water depth, nor have we firmly identified any characters to establish relative age. Where subbottom reflectors are observed over some of the blocks, they appear to match the surrounding sea floor in thickness---generally no more than 10 m. No overlapping of sediment onto the sides of the blocks was recorded. In general, the larger blocks prevent acoustic

penetration into the sediment under them, causing an acoustic shadow below the block surface; smaller blocks appear as velocity "pull-ups" in the air-gun profiles.

The seismic-reflection profiles also showed the existence of two smaller and older slides underlying the section on which the Wailau and Nuuanu slides rest (Figure 20). At about 0.1 sec round-trip travel time below the sea floor (perhaps 70 to 90 m of sediment), there are zones of hummocky topography and chaotic bedding along both the eastern and western margins of the big slides. The western slide deposit (north of western Oahu) forms a saddle-like swell that interrupts the Hawaiian Trough, just as the Wailau and Nuuanu slides interrupt the Trough north of Molokai.

**Other Gravitational Slides.** Several other landslides were also imaged, but we have few data from this cruise to describe them. They range widely in size. The largest are giants apparently comparable with the Nuuanu and Wailau slides. Two examples form broad bathymetric ridges that extend northeast and south from Kauai. Even though we suspected, from the subaerial geology of Kauai, that giant landslides had greatly affected the growth of the island, it seemed equally possible that these ridges were ancient rift zones. When one of our survey lines grazed the northeastern ridge, however, we found the characteristically chaotic large blocks of a giant landslide. That whetted our interest such that, when we steamed to the lee of Kauai to take GLORIA out of the water, we deliberately crossed the southern ridge in order to see if it too was a landslide. It is a slide of apparently immense size.

We also found sets of rotated, transversely-elongate fault blocks (of the Hilina type) along the north side of Haleakala Ridge and the southeast flank of Niihau. Among the more interesting 'small' slides that we found were a strikingly elongate and regular train of features that might be fault blocks on the floor of the Hawaiian Trough east of the submarine Wailau ridge and lobate features that may represent thick debris-flow lobes west of that same ridge. The latter lobes resemble those found locally along the base of Kilauea's Hilina fault system during earlier GLORIA surveying.

**Submerged Reefs.** We failed to find more sets of multiple submerged reefs like those found in 1986 along the crest of the Haleakala Ridge and elsewhere around the southern islands of the Hawaiian Ridge (Holmes et al., 1987; Moore, 1987; Moore and Fornari, 1984). We expected to see such multiple terraces north of Maui but instead found only a few hints that such terraces might exist. GLORIA had also failed earlier to image well the spectacular terraces west of Kohala, even though those examples are well known from bathymetry, dredging, and submersible observations. Various factors could account for the apparent absence of multiple terraces north of Maui: (1) Some shallow terraces might have escaped detection because of a velocity inversion in the water column that seems to be especially prominent in that area. (2) Some terraces might have escaped imaging under nadir. (3) Some terraces could have slumped away into the Hawaiian Trough, especially if the step faults imaged in that area long postdate the growth of the Haleakala shield.

We did image broad submerged terraces at several places around the southern, eastern, and northern shores of Oahu. In most places only one or two terraces were well developed, but in

some places there were signs that smaller terraces might occur at two or three additional levels. We found no clear signs of terraces postdating the giant landslides north of Molokai and east of Oahu. Late in the cruise, we saw some evidence for multiple terrace levels around the long submarine ridge extending northwestward from Oahu, and it appeared that these terraces postdated one or more giant landslides off that ridge. Subsequent survey legs will complete the examination of this ridge, but until these data are available, the number of terraces and their temporal relationship to landsliding cannot be determined.

**Young lava flows between Oahu and Kauai.** During our final transit to the lee of Kauai, GLORIA imaged three high-backscatter lava flows northwest of Oahu. These flows occur on the southern flank of the submarine saddle between Oahu and Kauai at depths of 3500 to 4500 m, and they appear to have spread mostly southward. Two of the flows are at least tens of kilometers long and extend beyond the limits of our single-image swath, but the third flow was entirely imaged within the swath. This third flow produced a peculiar 3.5-kHz record: the margins of the feature were less than 15-20 m thick, but its center was a high-standing plateau more than 100 m high. We suspect that we crossed the vent edifice, which remained unseen in the nadir part of the GLORIA image. Future surveys will have to confirm the existence of such an edifice. This flow looked extremely young, judging from its very high backscatter and the intricate details along its margin. It may be an historic flow: on May 22, 1956 a patch of discolored water, sulfurous odor, and dead sea animals were reported in this area, and basaltic pumice washed ashore on Oahu a few days later (Macdonald, 1959, p. 66-68). Those phenomena and this lava flow could all be the products of a single submarine eruption. If so, that eruption could be valuable for measuring rates of hydration and sedimentation in fairly deep water near the Hawaiian Ridge.

These very young lava flows on the Hawaiian Ridge are similar in age not only to the rejuvenated-stage lavas of Kauai and Oahu but also to the more extensive young flows to the north on the Hawaiian Arch. All of these young lava flows could represent peripheral eruptions around the Hawaiian hotspot. Instead of being merely the last dregs of Hawaiian activity in the wake of the hotspot, the rejuvenated-stage lavas could represent a more general pattern of volcanism occurring around the hotspot in all directions. If so, the discovery of these various young lava fields should lead to significant revisions in our understanding of the Hawaiian volcanic system.

**A possible Hawaiian shield volcano northwest of Waianae.** The giant landslides, submerged terraces, and recent volcanism along the rather large ridge west-northwest of Oahu cause us to suspect that this ridge is the remnant of a formerly much larger subaerial volcano belonging to the Hawaiian chain, a volcano separate from the Waianae Volcano. This suspicion should be testable through K-Ar dating; if it is a separate volcano, it should yield K-Ar dates intermediate between those of Waianae and Kauai.

## REFERENCES CITED

- Atwater, T.M., 1989, Plate tectonic history of the Northeast Pacific and western North America, *in* E.L. Winterer, D.M. Hussong, and R.W. Decker, eds, Decade of North American Geology, vol. N, The Eastern Pacific Region, Geological Society of America, Boulder, Colorado.
- Atwater, T. and Menard, H. W., 1970, Magnetic lineations in the northeast Pacific: Earth and Planetary Science Letters, v. 7, p. 445-450.
- Chase, T. E., Menard, H. W., and Mammerickx, J., 1970, Bathymetry of the North Pacific, chart 8 of 10: Institute of Marine Resources Technical Report Series TR-6.
- Chase, T.E., Miller, C.P., Seekins, B.A., Normark, W.R., Gutmacher, C.E., Wilde, P., and Young, J.D., 1981, Topography of the southern Hawaiian Islands: U.S. Geol. Survey Open-File Report 81-120, 3 sheets.
- Chavez, P. S., Jr., 1986, Processing techniques for digital sonar images from GLORIA: Photogrammetric Engineering and Remote Sensing, v. 52, p. 1133-1145.
- Clague, D. A. and Dalrymple, G. B., 1975, Cretaceous K-Ar ages of volcanic rocks from the Musicians Seamounts and the Hawaiian Ridge: Geophys. Research Letters, v. 2, p. 305-308.
- Clague, D.A., Holcomb, R.T., Torresan, M.E., and Ross, S.L., 1989, Shipboard report for Hawaii ground-truth cruise F11-88-HW, 25 Oct.-7 Nov., 1988: U.S. Geol. Survey Open-File Report 89-109, 37 p.
- Clague, D.A., Moore, J. G., Torresan, M.E., Holcomb, R.T., and Lipman, P.W., 1988, Shipboard report for Hawaii GLORIA ground-truth cruise F2-88-HW, 25 February--9 March 1988: U.S. Geological Survey Open-File Report 88-292, 54 p.
- Damuth, J. E., Kolla, V., Flood, R. D., Kowsmann, R. O., Monteiro, M. C., Gorini, M. A., Palma, J. C., and Belderson, R. H., 1983, Distributary channel meandering and bifurcation patterns on the Amazon deep-sea fan as revealed by long-range side-scan sonar: Geology, v. 11, p. 94-98.
- Dana, J. D., 1849, Geology. United States Exploring Expedition, 1838-1842, vol. 10, 756 pp.
- EEZ SCAN 84 Scientific Staff, 1986, Atlas of the Exclusive Economic Zone, western conterminous United States: U.S. Geol. Survey Misc. Investigation Series I-1792, 152 p.
- EEZ SCAN 85 Scientific Staff, 1987, Atlas of the U. S. Exclusive Economic Zone, Gulf of Mexico and Eastern Caribbean Areas: U. S. Geol. Survey Misc. Investigation Series I-1864-A, 162p.
- Flood, R. D., and Damuth, J. E., 1987, Quantitative characteristics of sinuous distributary channels on the Amazon deep-sea fan: Geol. Soc. American Bull., v. 98, p. 728-738.
- Haxby, W. F., 1987, Gravity field of the world's oceans: World Data Center for Marine Geology and Geophysics, Report MGG-3, National Oceanic and Atmospheric Admin., National Geophys. Data Center, Boulder, CO.
- Holcomb, R.T., 1976, Complexity and hazards of Hawaiian shield volcanoes: Geol. Soc. Amer. Abstracts with Programs, p. 920-921.

- Holcomb, R.T., 1985, The caldera of East Molokai volcano, Hawaiian Islands: National Geographic Society Research Reports, v. 21, 1980-1983, p. 81-87.
- Holcomb, R. T., Moore, J. G., Lipman, P. W., and Belderson, R. H., 1988, Voluminous submarine lava flows from Hawaiian volcanoes: *Geology*, v. 16, p. 400-404.
- Holmes, M.L., Moore, J.G., Holcomb, R.T., and Belderson, R.H., 1987, Preliminary cruise report, Research Vessel FARNELLA, Windward Hawaii, F5-86-HW: U.S. Geological Survey Administrative Report.
- Karl, H. A., Gardner, J. V., and Huggett, Q., 1987, GLORIA images of Zhemchug Canyon and Bering channel-fan system, Bering Sea: *Geologic Studies in Alaska by the U. S. Geological Survey during 1986*, ed. by T. D. Hamilton and J. P. Galloway, U. S. Geological Survey Circular 998, p. 147-151.
- Kastens, K. A., 1984, Earthquakes as a triggering mechanism for debris flows and turbidites on the Calabrian Ridge: *Marine Geol.*, v. 55, p. 13-33.
- Kastens, K. A. and Shor, A. N., 1985, Depositional processes of a meandering channel on Mississippi Fan: *American Association of Petroleum Geologists Bulletin*, v. 69, p. 190-202.
- Kastens, K. A. and Shor, A. N., 1986, Evolution of a channel meander on the Mississippi Fan: *Marine Geology*, v. 71, p. 165-175.
- Langford, S. A. and Brill, R. C., 1972, Giant submarine landslides on the Hawaiian Ridge: A rebuttal; *Pacific Science* 26, p. 254-258.
- Lipman, P.W., Normark, W.R., Moore, J.G., Wilson, J.B., and Gutmacher, C.E., 1988, The giant submarine Alika debris slide, Mauna Loa, Hawaii: *Journal of Geophysical Research*, v. 93, p. 4279-4299.
- Macdonald, G. A., 1959, The activity of Hawaiian volcanoes during the years 1951-1956: *Bulletin Volcanologique, Series 2*, v. 22, p. 3-70.
- MacGregor, B.A., Kappel, E.S., Wilson, J.B., Campbell, J., Trincardi, F., Whittington, R.J., and Mayer, W., 1989, Cruise Report, Hawaiian GLORIA Leg 6, F10-88-HW, U.S. Geological Survey Open-File Report (in review).
- Menard, H. W., and Atwater, T., 1968, Changes in direction of sea floor spreading: *Nature*, v. 219, p. 463-467.
- Menard, H. W., and Atwater, T., 1969, Origin of fracture zone topography: *Nature*, v. 222, 1037-1040.
- Moore, J.G., 1964, Giant submarine landslides on the Hawaiian Ridge: U.S. Geol. Survey Prof. Paper 501D, p. D95-D98.
- Moore, J.G., 1987, Subsidence of the Hawaiian Ridge: U.S. Geol. Survey Prof. Paper 1350, p. 85-100.
- Moore, J.G., and Campbell, J.F., 1987, Age of tilted reefs, Hawaii: *Journal Geophysical Research*, v. 92, p. 2641-2646.

- Moore, J. G. and Moore, G. W., 1984, Deposit from a giant wave on the island of Lanai, Hawaii: *Science*, v. 226, p. 1312-1315.
- Moore, J.G., and Fornari, D.J., 1984, Drowned reefs as indicators of the rate of subsidence of the Island of Hawaii: *Jour. Geol.*, v. 92, p. 752-759.
- Normark, W. R., Lipman, P. W., and Moore, J. G., 1979, Regional slump structures on the west flank of Mauna Loa volcano, Hawaii (abstract): Hawaii Symposium on Intraplate Volcanism and Submarine Volcanism, International Assoc. of Volcanol. and Chem. of the Earth's Interior, Hilo, Hawaii.
- Normark, W.R., Lipman, P.W., Wilson, J.B., Jacobs, C.L., Johnson, D.P., and Gutmacher, C.E., 1987, Preliminary Cruise Report, Hawaiian GLORIA Leg 2, F6-86-HW, November 1986, U.S. Geological Survey Open-File Report 87-298, 42 p.
- Rea, D. K., 1970, Changes in structure and trend of fracture zones north of the Hawaiian Ridge and relation to sea-floor spreading: *Jour. Geophysical Res.*, v. 75, p. 1421-1430.
- Rea, D. K. and Naugler, F. P., 1970, Musicians Seamounts province and related crustal structures north of the Hawaiian Ridge: *Marine Geology*, v. 10, p. 89-111.
- Sager, W.W., and Pringle, M.S., 1987, Paleomagnetic constraints on the origin and evolution of the Musicians Seamounts, central Pacific ocean: *in* B. Keating, P. Fryer, and G. Goehrlert, eds, *Seamounts, Islands, and Atolls: Geophysical Monograph 43*, American Geophysical Union, Washington, D.C, p. 133-162.
- Searle, R. C., 1983. Multiple, closely-spaced transform faults in fast-slipping fracture zones. *Geology*, 11, 607-610.
- Searle, R. C., 1986. GLORIA investigations of oceanic fracture zones: comparative study of the transform fault zone. *J. Geol. Soc.*, London, v. 143, p. 743-756.
- Somers, M. L., Carson, R. M., Revie, J. A., Edge, R. H., Barrow, B. J., and Andrews, A. G., 1978, GLORIA II--an improved long range sidescan sonar: *Proceedings of IEE/IERE Subconf. on Ocean Instruments and Communication; Oceanology International*, B. P. S. Pub. Ltd., London, P. 16-24.
- Spiess, F. N., Luyendyk, B. P., Larson, R. L., Normark, W. R., and Mudie, J. D., 1969, Detailed geophysical studies on the northern Hawaiian Arch using a deeply towed instrument package, *Marine Geology*, v. 7, p. 501-527.
- Tamsett, D., and Searle, R. C., 1988. Structure and development of the midocean ridge plate boundary in the Gulf of Aden: Evidence from GLORIA sidescan sonar. *Jour. Geophys. Res.*, v. 93, p. 3157-3178.
- Torresan, M.E., Shor, A.N., Wilson, J.B., and Campbell, J., 1989, Cruise Report, Hawaiian GLORIA Leg 5, F5-88-HW: U.S. Geological Survey Open-File Report 89-XXX, 56 p.
- Turcotte, D.L., 1974, Are transform faults thermal contraction cracks?: *Journal Geophysical Research*, v. 79, p. 2573-2577.
- Turcotte, D.L., and Oxburgh, E.R., 1973, Mid-plate tectonics: *Nature*, v. 244, p. 337-339.

Wallin, B. H. 1982, The northern Hawaiian Deep and Arch: Interpretation of geologic history from reflection profiling and echo character mapping: MS thesis, University of Hawaii, Honolulu, 133 p.

White, R. S., , Spence, G. D., Fowler, S. R., McKenzie, D. P., Westbrook, G. K., and Bowen, A. N., 1987, Magmatism at rifted continental margins: *Nature*, v. 330, p. 439-444.

Wilde, P., Chase, T.E., Normark, W.R., Thomas, J.A., and Young, J.D., 1980, Oceanographic data off southern Hawaiian Islands: Lawrence Berkeley Lab. Earth Science Div. Publ. 359.

Winterer, E.L., and Sandwell, D.T., 1987, Evidence from en-echelon cross-grain ridges for tensional cracks in the Pacific plate: *Nature*, v. 329, p. 534-537.

## FIGURE CAPTIONS

- Figure 1. Major geographic features around the Hawaiian Islands showing location of area covered by GLORIA legs F3-88-HW and F4-88-HW; modified from Chase et al., 1970. Areas shown on Figures 2 and 3 are outlined.
- Figure 2. Track chart for F3-88-HW, showing location of Figures 6, 7, 13, and 14.
- Figure 3. Track chart for F4-88-HW, showing location of Figures 11 and 17 through 20.
- Figure 4. Location of expendable bathythermograph stations taken during legs F3 and F4; see listing in text.
- Figure 5. Profiles of mean and maximum dn values for GLORIA passes F3/1 (night) and F3/2 (day), over pelagic sediment with lineated basalt outcrops along abyssal hills and fracture zones; and pass F4/39 recorded over pelagic sediments with 30% recent lava flows, after the GLORIA gain settings were changed at 0145/086.
- Figure 6. Tectonic elements of the Molokai Fracture Zone. Letters A through D indicate separate fracture zone segments discussed in the text. See Figure 2 for location.
- Figure 7. GLORIA sonograph showing ENE-WSW lineaments inferred to be fossil transform fault traces. The lineaments normally consist of north-facing scarps (revealed as narrow, bright reflectors on north-looking sonographs or linear shadows on south-looking ones) or colinear terminations of curved spreading fabric. See Figure 2 for location.
- Figure 8. Projection of Molokai Fracture Zone bands A and B westwards, showing where they are thought to continue beneath the Hawaiian Ridge to join bands E and F southwest of Oahu. The thick line between Maui and Hawaii shows the line of section in Figure 10.
- Figure 9. Cartoon showing proposed changes in spreading direction, plate boundary structure, and resultant magnetic-polarity pattern around the Molokai Fracture Zone. Arrows in A, B indicate relative directions of plate motion; shading in C, D, E indicates sea floor having normal magnetic polarity.
- A. Inferred geometry of spreading segments and fracture zones prior to change of spreading direction, with major transform faults a'b and c'd offsetting the spreading axis along the Molokai North and South fracture zones.
- B. General situation after change of spreading direction, with rhomboids aa'b'b and cc'd'd having opened up at the sites of the old Molokai North and South transform faults.
- C. Spreading center and pattern of magnetization shortly after change in spreading direction and polarity transition at about 84 Ma. Long spreading segments have broken up into short en echelon segments, and transform faults have become leaky.
- D. Reorganized spreading center about at about 80 Ma, 4 Ma after change in spreading direction. Long ridge segments have propagated perpendicular to new spreading direction, and leaky transforms have been replaced by chains of short new transforms and spreading segments. The southern rhomboid is drawn with a single spreading center within it, but the northern one is shown with two segments separated by an intermediate transform. Details of the new plate boundary within the rhomboids are uncertain. This latter transform and one of the spreading centers might in time disappear.
- E. Pattern of seafloor magnetization at about 70 Ma, after the change in spreading direction. Superimposed for reference are modern islands of Hawaiian Ridge. Dashed lines to left of islands are observed strands E, F of fracture zone; dotted lines are extrapolations of strands

observed east and west of Ridge. Only the area to left of heavy curved line is included in the GLORIA surveys.

Figure 10. Longitudinal cross-section of Hawaiian Ridge from Haleakala to Kohala, along the line shown in Figure 8. The topographic profile is well determined, but the base of the Ridge is inferred only approximately. Buried faults of the Molokai Fracture Zone are projected into this plane from their positions farther east.

Figure 11. Geologic map of the Hawaiian Arch volcanic field imaged during leg F4-88-HW. Although the other morpho-stratigraphic units are shown in correct temporal order in the explanation, the vent edifices have a wide range of ages, probably extending from Cretaceous to Holocene.

Figure 12. Regional bathymetric map, with linear volcanic ridges imaged during F4-88-HW outlined in black; adapted from Chase et al., 1970;1981. Also shown are the trends of the Molokai Fracture Zone. Heavy dashed line shows axis of Hawaiian Arch.

Figure 13. GLORIA images of adjacent parallel passes from leg F3 (pass nos. 002 and 008), showing channel in the area common to both images. See Figure 2 for location.

Figure 14. Geologic map of a part of the Molokai Fracture Zone, showing east-trending ridges (scored by ancient north-trending structures of the spreading center) separated by valleys partly filled by sediment (stippled pattern). Channel-like feature shown by wide black band, continuous where well-imaged near 153°W and broken where less well defined. Numbers indicate 3.5-kHz profile lines 1 through 6 shown in Figure 15. Note hills H, along edge of channel, and locality R where channel is edged by low levee-like ridges. See Figure 2 for location.

Figure 15. 3.5-kHz reflection profiles along lines 1 through 6 of Figure 14, across the channel and its extensions. Depth to channel is indicated on each profile.

Figure 16. Longitudinal profiles along the channel-like feature and floors of adjacent valleys. Locations given in Figure 14.

Figure 17. GLORIA image across western margin of slide deposit north of Oahu. Location given in Figure 3.

Figure 18. Single-channel monitor record of seismic-reflection profile across western margin of the slide deposit north of Oahu (along nadir of GLORIA image in Figure 17). Profile location given in Figure 3.

Figure 19. Map showing imaged blocks of the combined Nuuanu and Wailau slide deposits. Location given in Figure 3.

Figure 20. Map summarizing salient features of the Nuuanu and Wailau slides and some other nearby slide deposits. Location given in Figure 3.

## APPENDIX I: EQUIPMENT SETTINGS AND COMMENTS

F3-88-HW; F4-88-HW

### 1. 3.5 kHz system

LSR (Recorder)	MODE	Continuous
	PAPER	150 lines/inch
	SWEEP	1 sec.
	PROGRAM	As required
	GAIN	Variable
	CONTRAST	Mid-range
	THRESHOLD	Low to mid-range
PTR Transceiver	GAIN	9 low (fixed; ramp control not active)
	POWER	0 db
	PULSE WIDTH	Controls not active
IOS Correlator	OUTPUT LEVEL	4
	ATTENUATOR	11.5

Fish depth compensation is set at 15 m. Instructions for the time and cruise id are in the manual provided.

### 2. 10-kHz System

MUFAX Recorder	ATTENUATOR	-6 (-12, -18 if needed)
	PULSE LENGTH	2.8 msec (5 if needed)
	TIME MARKS	6 min. intervals
	FISH DEPTH	6 m (controls 6 x 1)
	GATING INT	6 sweeps
	SWEEP	2 sec.
	SCALE	1500 m/sweep
	PROGRAM	Edge or center key; allows scale changes of 1 sec. intervals
	TVG	Can be used to suppress the outgoing pulse

Note: The TVG is normally on when the GATING is on and vice versa.

### 3. Seismic reflection system (two channel)

Sound source	AIR GUN	160 in <sup>3</sup>
Receiver	2 CHANNEL	50 m active sections
LSR (Recorder)	DISPLAY	Normal
	STYLUS SCAN	2 sec.
	PAPER	120 lines/inch
	MEMORY SWEEP	6 sec.
	FILTER	In
	POLARITY	+

GAIN	4 to 5
CONTRAST	-30
THRESHOLD	5 (FWC as needed)

Krohn-Hite Filter	20 -80 Hz
-------------------	-----------

Amplifier	Not a seismic unit (ours was not functioning properly). We used a simple oscilloscope differential amplifier (AM 502).
-----------	--

MASSCOMP	RECORD LENGTH	6 sec.
	GAIN (prefilter)	0 db
	GAIN (postfilter)	6, 12, or 18 db depending upon water depth and seafloor reflectivity.
	DELAY	Variable

4. Gravimeter

Standard operation; watchstander only checks gravity and spring tension values on the hour and marks the paper record with time, course, speed once an hour as part of the routine log entry. All adjustments or changes to operation will be handled by electronics tech or the designated navigator.

5. Magnetometer

Standard operation; watchstander checks field value on the hour; logging procedures and equipment changes are the same as for the other potential field data.

6. XBT

One XBT probe every day about 1500 L. The NOAA recording unit has complete instructions for launching, plotting, and transmitting the data. Use a T-7 probe (750 m) about once a week and T-4 or T-6 probes (450 m) otherwise.

APPENDIX 2: SUMMARY OF GLORIA PASSES FOR F3-88-HW

<u>PASS #</u>	<u>START TIME</u>	<u>FINISH TIME</u>	<u>FILE #</u>	<u>TAPE #</u>	<u>COMMENTS</u>
1	0948/072	1500/072	01	01	Logger time 10 hrs fast
2	1500/072	2100/072	02	01	Logger time 10 hrs fast
3	2100/072	2255/072	03	01	Logger time 10 hrs fast
4	2255/072	0400/073	04	01	'0' errors
5	0400/073	0930/073	05	01	"Forced" to start replay
6	0930/073	1500/073	06	01	"Forced" to correct time
7	1500/073	2100/073	07	01	No errors
8	2100/073	0300/074	08	01	No errors
9	0300/074	0900/074	09	01	No errors
10	0900/074	1500/074	10	01	No errors
11	1500/074	2100/074	11	01	No errors
12	2100/074	0300/075	12	01	No errors
13	0300/075	0900/075	13	01	No errors
14	0900/075	1500/075	14	01	No errors
15	1500/075	2100/075	15	01	No errors
16	2100/075	0300/076	16	01	No errors
17	0300/076	0900/076	01	02	No errors
18	0900/076	1500/076	02	02	No errors
19	1500/076	1600/076	03	02	End of leg; shut down

APPENDIX 3: SUMMARY OF GLORIA PASSES FOR F4-88-HW

<u>PASS #</u>	<u>START TIME</u>	<u>FINISH TIME</u>	<u>FILE #</u>	<u>TAPE #</u>	<u>COMMENTS</u>
1	0249/078	0800/078	01	03	First pass of F4-88-HW
2	0800/078	1400/078	02	03	No errors
3	1400/078	2000/078	03	03	No errors
4	2000/078	0200/079	04	03	No errors
5	0200/079	0800/079	05	03	No errors
6	0800/079	1400/079	06	03	No errors
7	1400/079	2000/079	07	03	No errors
8	2000/079	2130/079	08	03	Stop to offload film crew
9	0143/080	0700/080	09	03	Restart after film crew left
10	0700/080	1300/080	10	03	No errors
11	1300/080	1900/080	11	03	No errors
12	1900/080	0100/081	12	03	No errors
13	0100/081	0700/081	13	03	No errors
14	0700/081	1300/081	14	03	No errors
15	1300/081	1848/081	15	03	Stopped to phase logging
16	1851/081	0000/082	16	03	Restart of logging
17	0000/082	0600/082	01	04	No errors
18	0600/082	1200/082	02	04	No errors
19	1200/082	1800/082	03	04	No errors
20	1800/082	0000/083	04	04	No errors
21	0000/083	0600/083	05	04	No errors
22	0600/083	1200/083	06	04	No errors
23	1200/083	1800/083	07	04	No errors
24	1800/083	0000/084	08	04	No errors
25	0000/084	0600/084	09	04	No errors
26	0600/084	1200/084	10	04	No errors
27	1200/084	1800/084	11	04	No errors
28	1800/084	0000/085	12	04	No errors
29	0000/085	0600/085	13	04	No errors
30	0600/085	1200/085	14	04	No errors
31	1200/085	1800/085	15	04	No errors
32	1800/085	0000/086	01	05	No errors
33	0000/086	0600/086	02	05	Port gain change at 0145
34	0600/086	1200/086	03	05	No errors
35	1200/086	1800/086	04	05	No errors
36	1800/086	0000/087	05	05	No errors
37	0000/087	0600/087	06	05	No errors
38	0600/087	1200/087	07	05	No errors
39	1200/087	1800/087	08	05	No errors
40	1800/087	0000/088	09	05	No errors
41	0000/088	0600/088	10	05	No errors
42	0600/088	1200/088	11	05	No errors
43	1200/088	1800/088	12	05	No errors
44	1800/088	0000/089	13	05	Cartridges 37/38 out of sequence
45	0000/089	0600/089	14	05	Cartridges 37/38 out of sequence
46	0600/089	1200/089	15	05	Cartridges 37/38 out of sequence
47	1200/089	1800/089	16	05	Cartridges 37/38 out of sequence

48	1800/089	0000/090	01	06	No errors
49	0000/090	0600/090	02	06	No errors
50	0600/090	1200/090	03	06	No errors
51	1200/090	1800/090	04	06	No errors
52	1800/090	0000/091	05	06	2135--write error
53	0000/091	0600/091	06	06	No errors
54	0600/091	1200/091	07	06	No errors
55	1200/091	1800/091	08	06	No errors
56	1800/091	0000/092	09	06	No errors
57	0000/092	0600/092	10	06	No errors
58	0600/092	1200/092	11	06	No errors
59	1200/092	1800/092	12	06	No errors
60	1800/092	0000/093	13	06	No errors
61	0000/093	0600/093	14	06	No errors
62	0600/093	1200/093	15	06	No errors
63	1200/093	1800/093	16	06	No errors
64	1800/093	0000/094	01	07	No errors
65	0000/094	0600/094	02	07	No errors
66	0600/094	1200/094	03	07	No errors
67	1200/094	1800/094	04	07	No errors
68	1800/094	0000/095	05	07	No errors
69	0000/095	0600/095	06	07	No errors
70	0600/095	1200/095	07	07	No errors
71	1200/095	1800/095	08	07	No errors
72	1800/095	2237/095	09	07	End of F4-88-HW

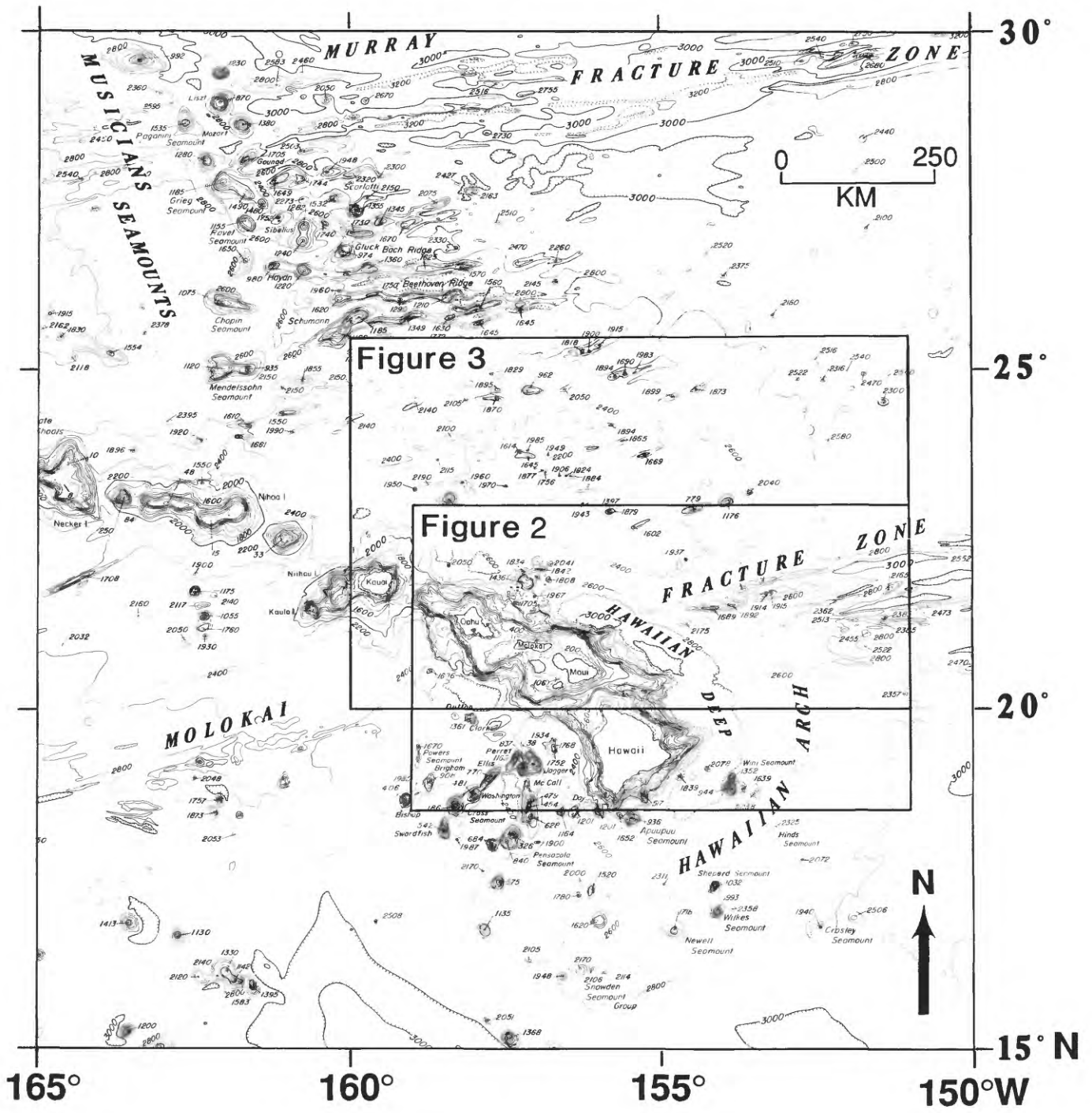


Figure 1

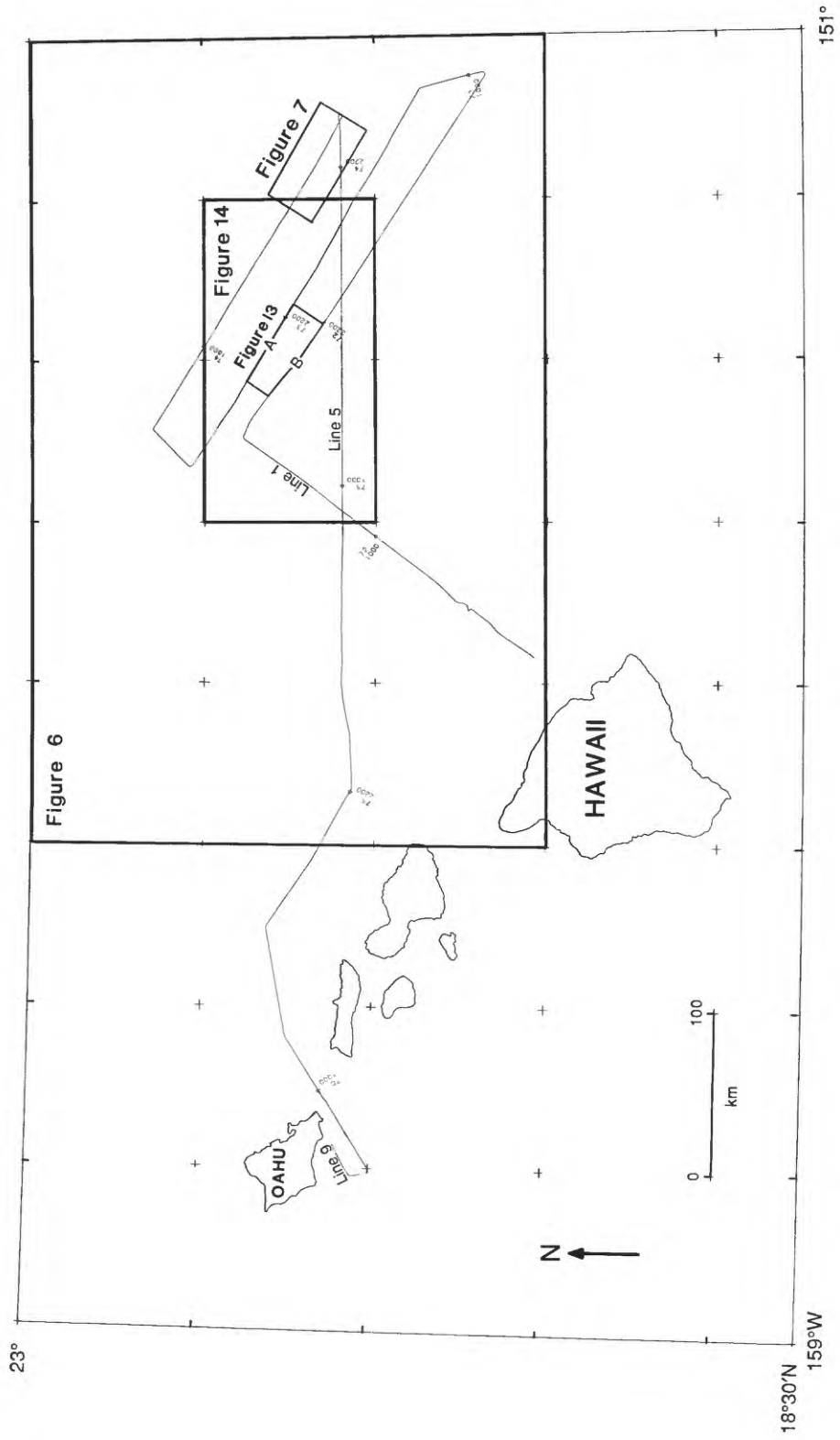


Figure 2

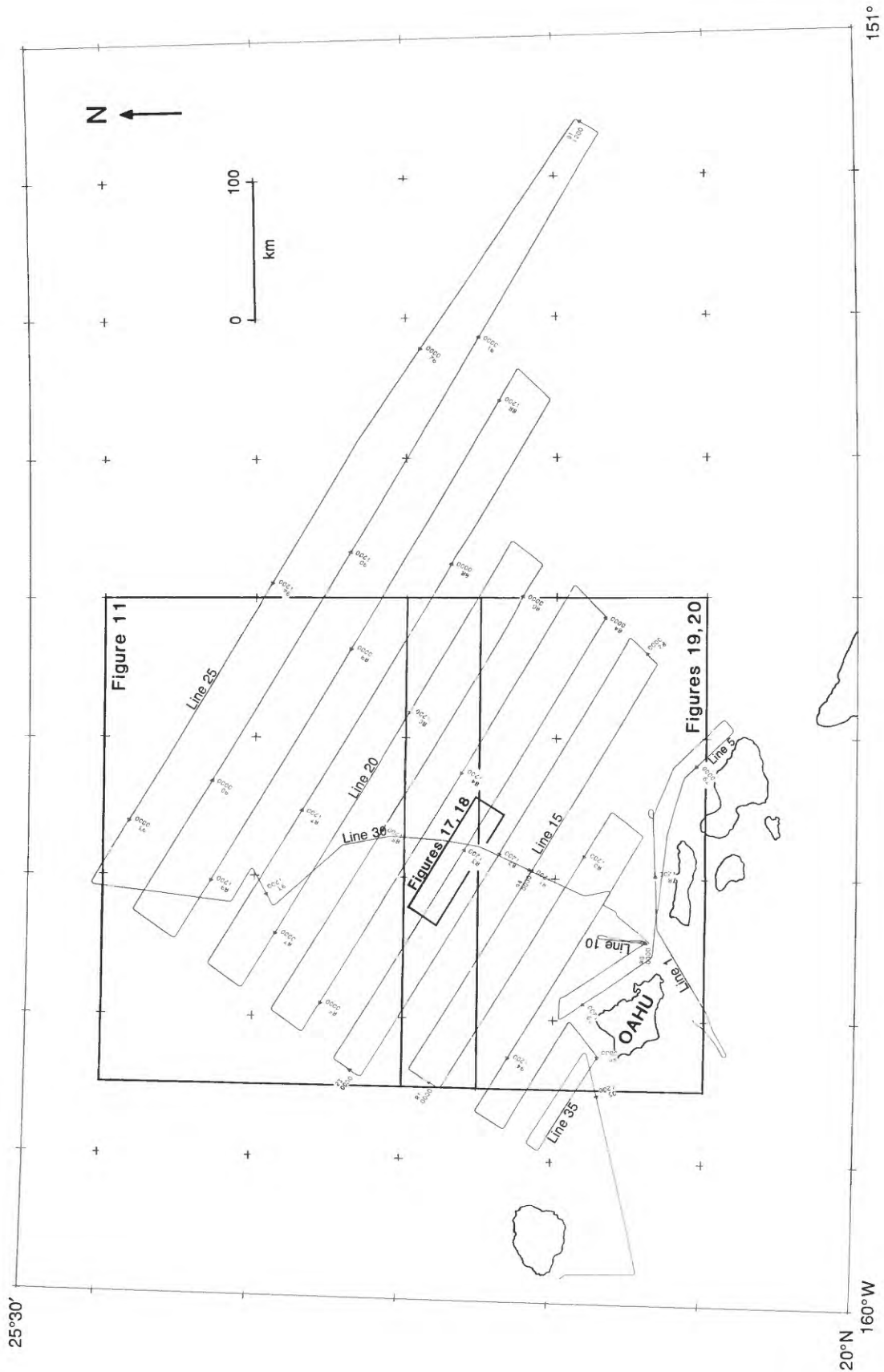


Figure 3

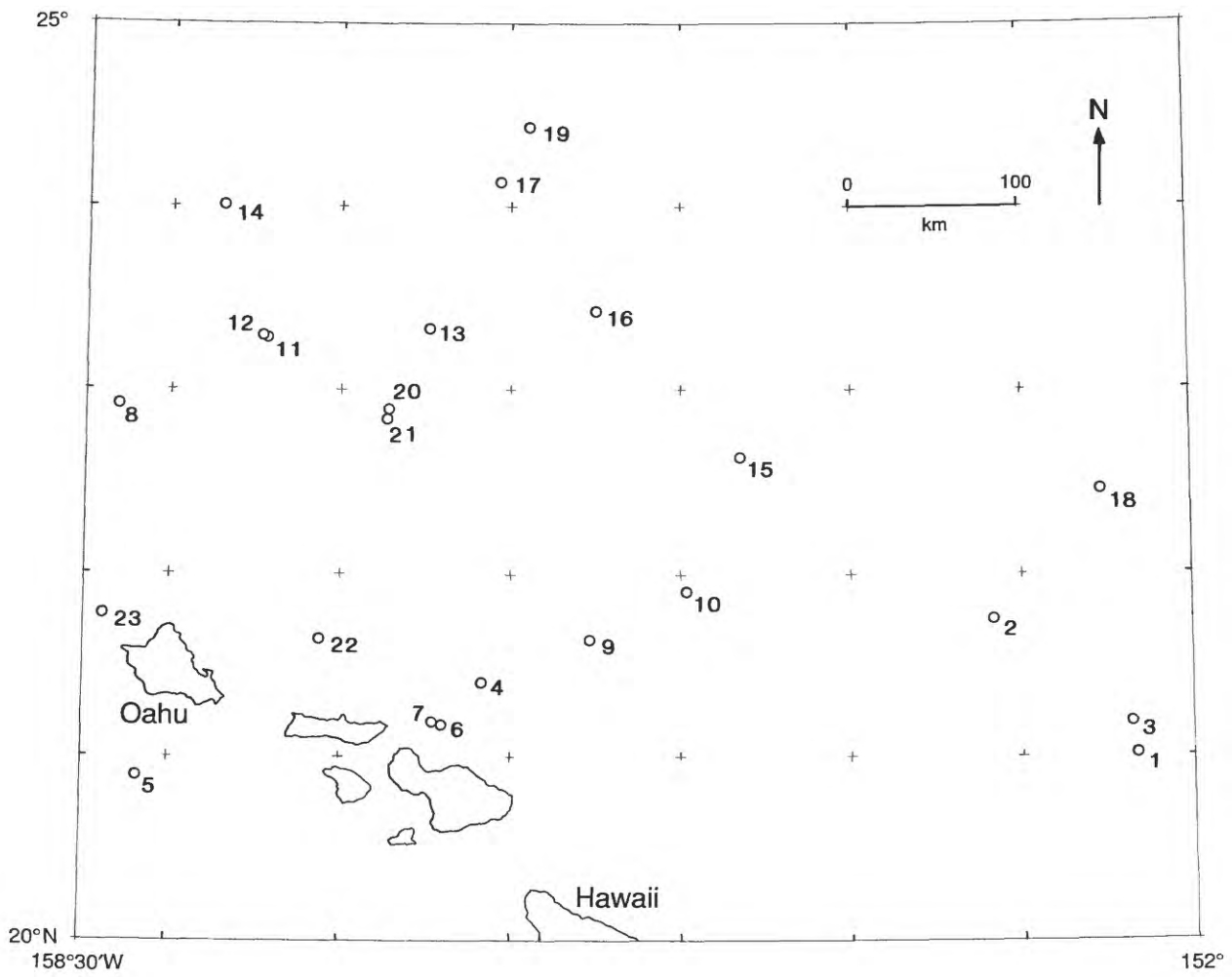


Figure 4

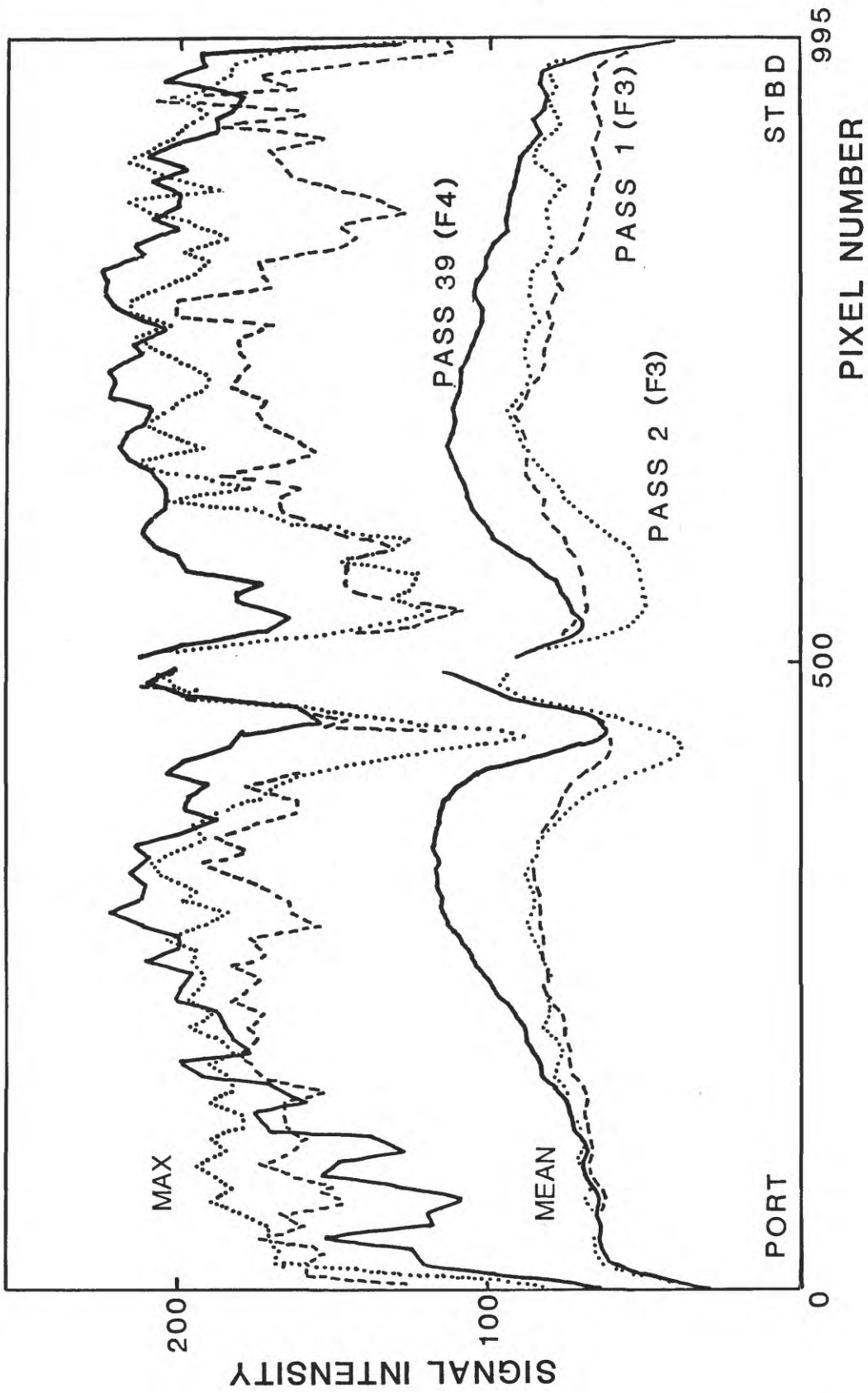


Figure 5

# TECTONIC LINEAMENTS OF THE MOLOKAI FRACTURE ZONE

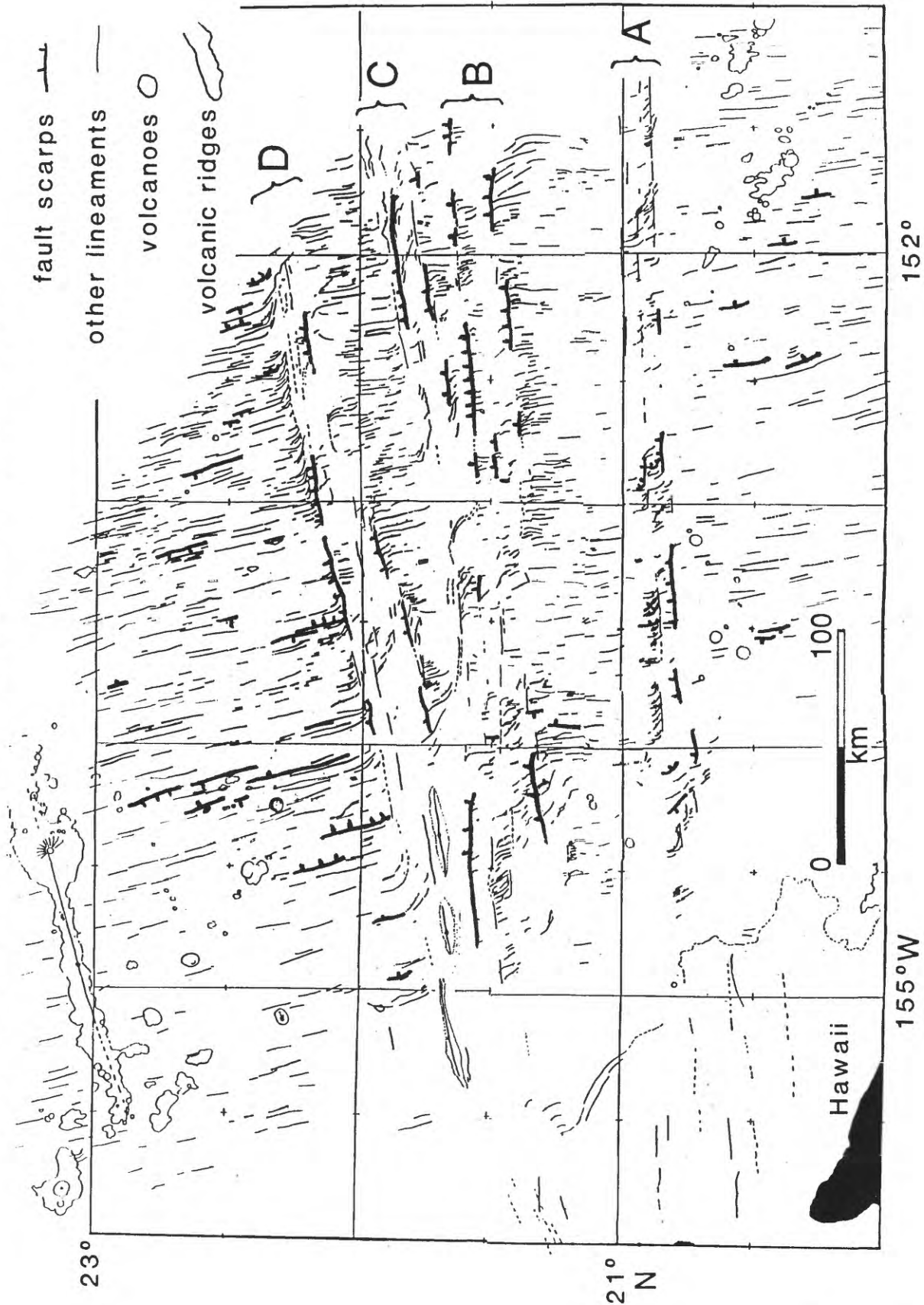


Figure 6

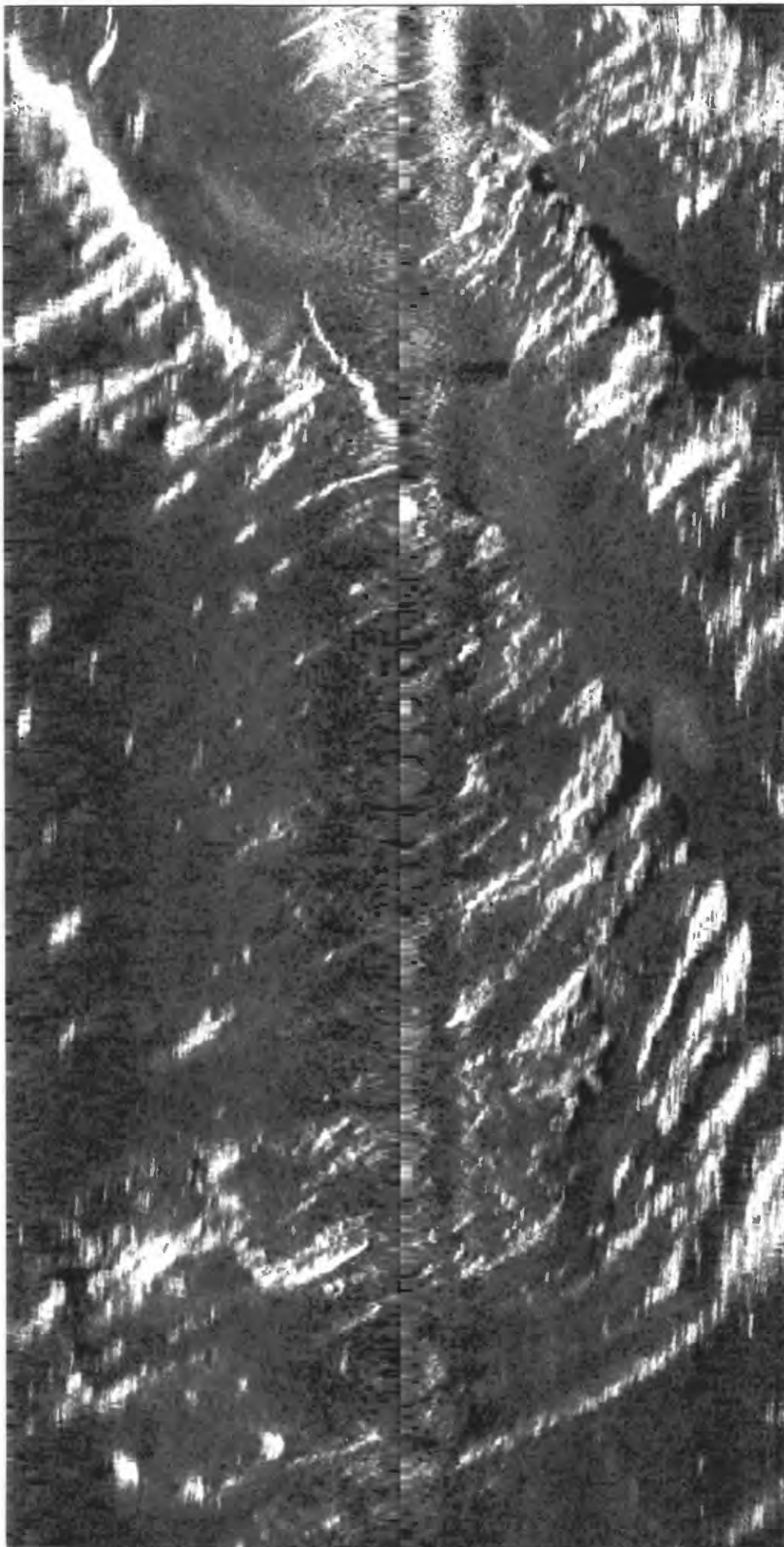


Figure 7

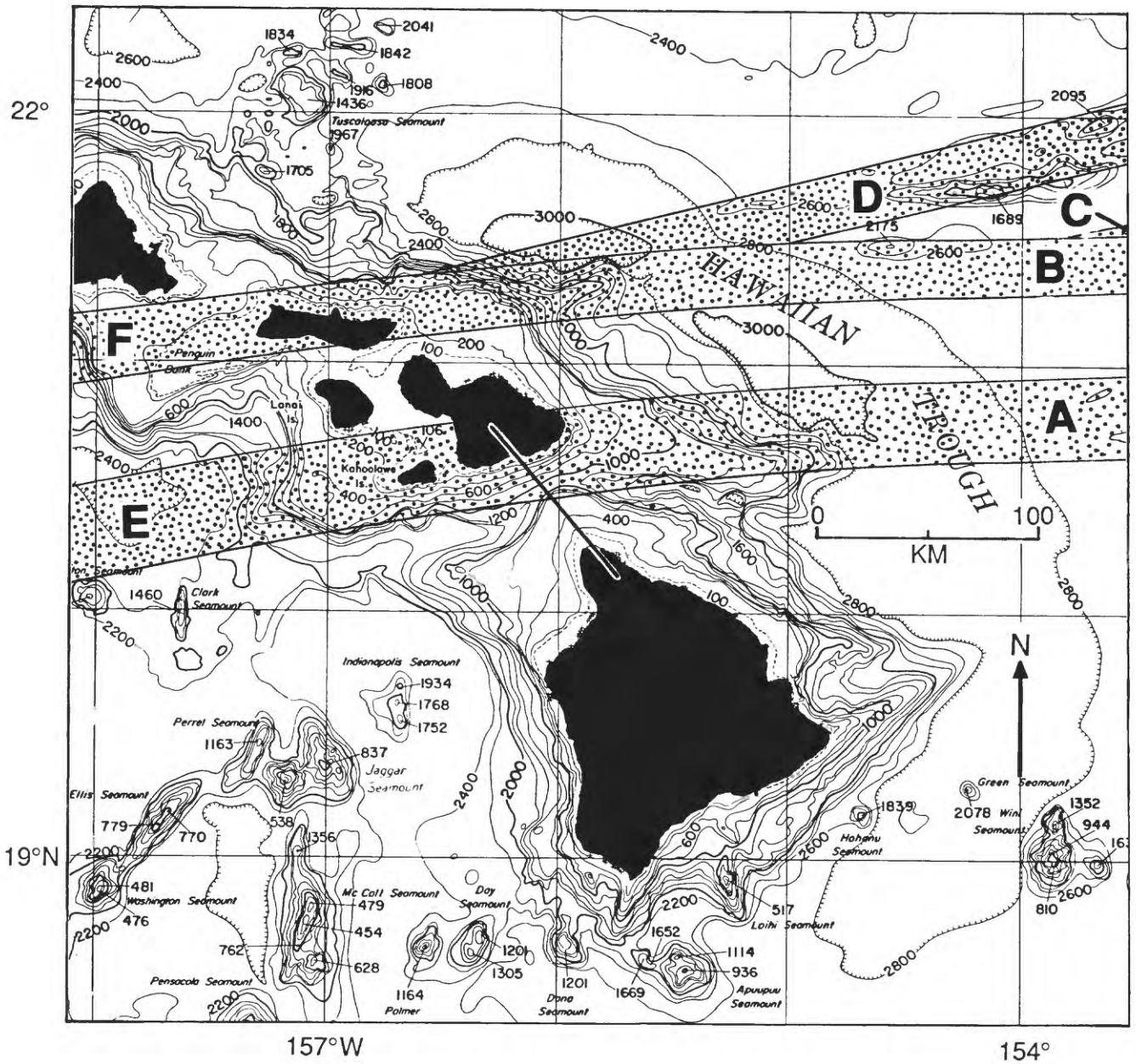
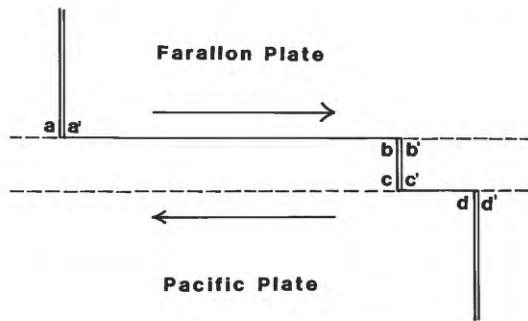
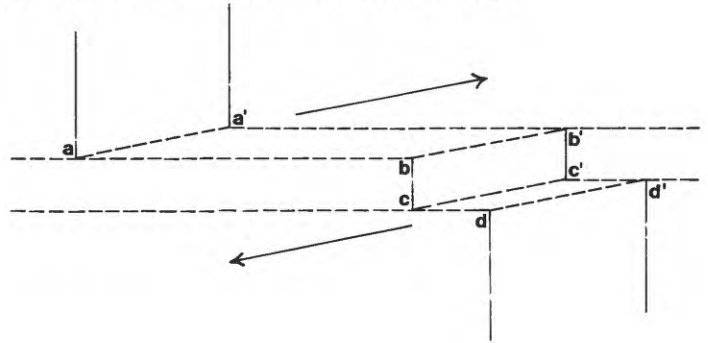


Figure 8

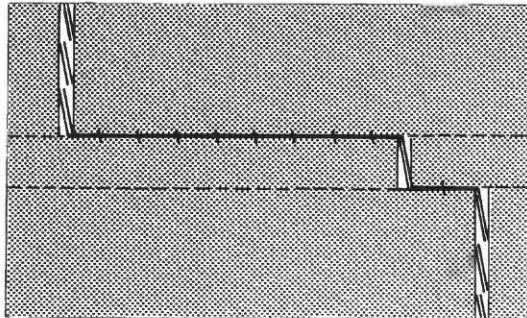
**A. Fracture zones before change**



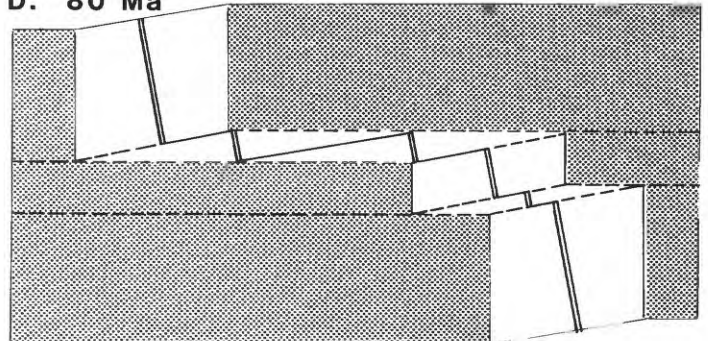
**B. Fracture zones after change**



**C. Shortly after 84 Ma**



**D. 80 Ma**



**E. 70 Ma, with later islands superimposed**

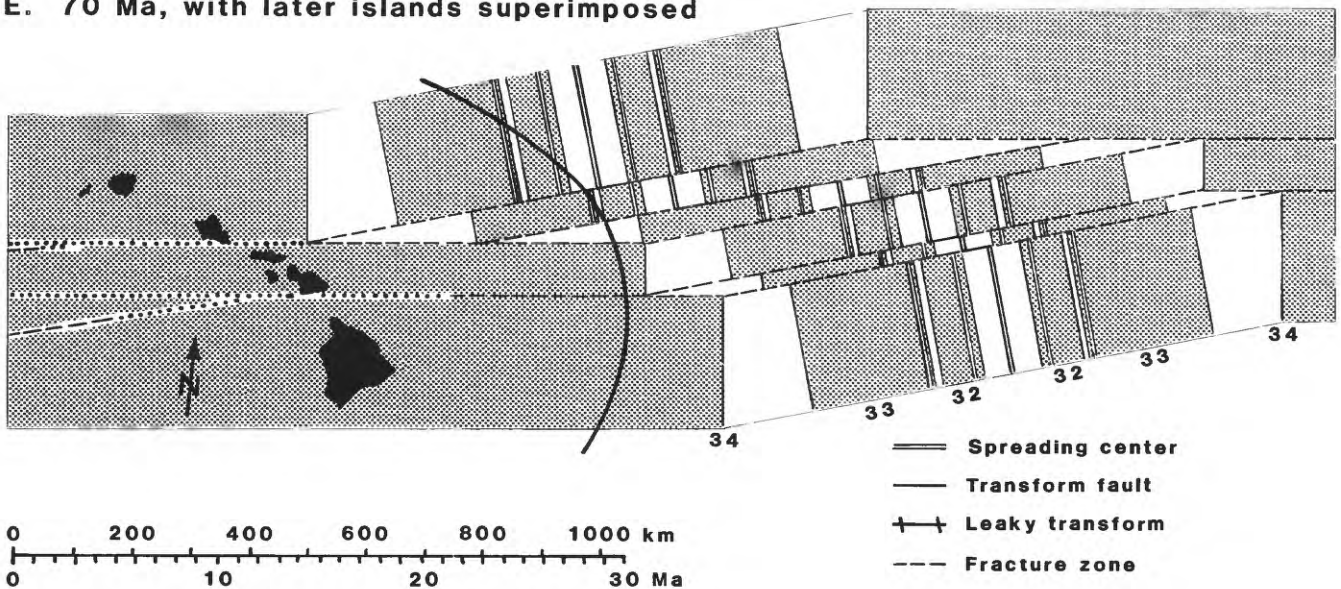


Figure 9

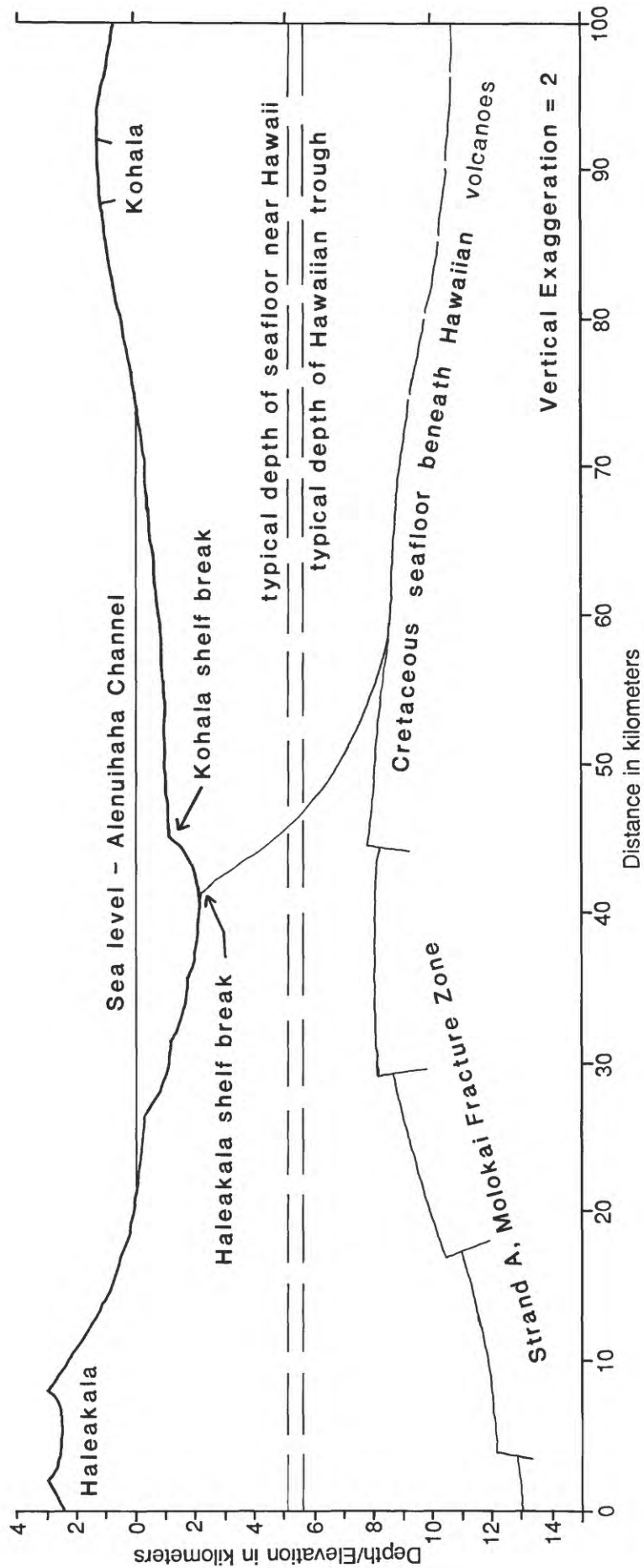


Figure 10

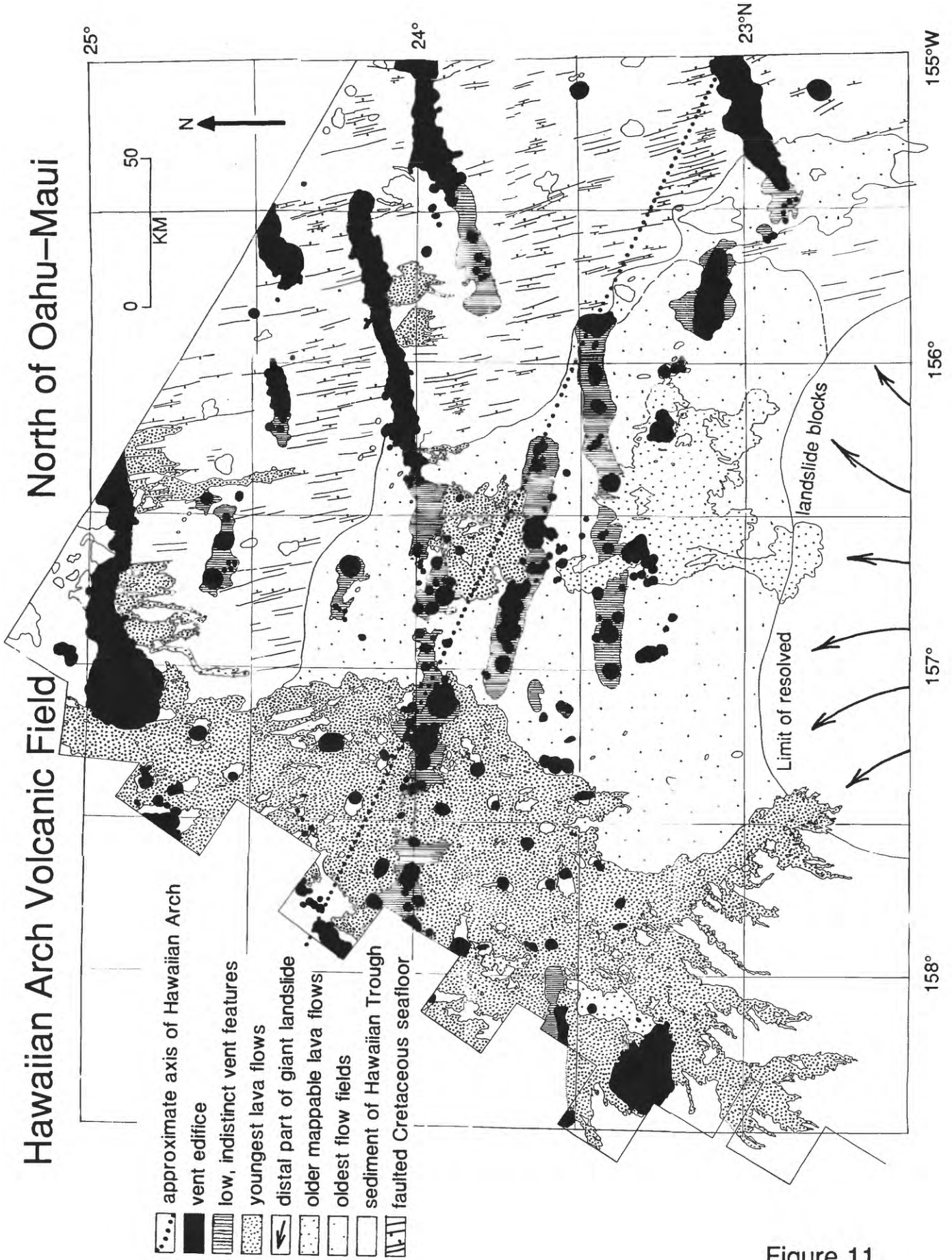


Figure 11

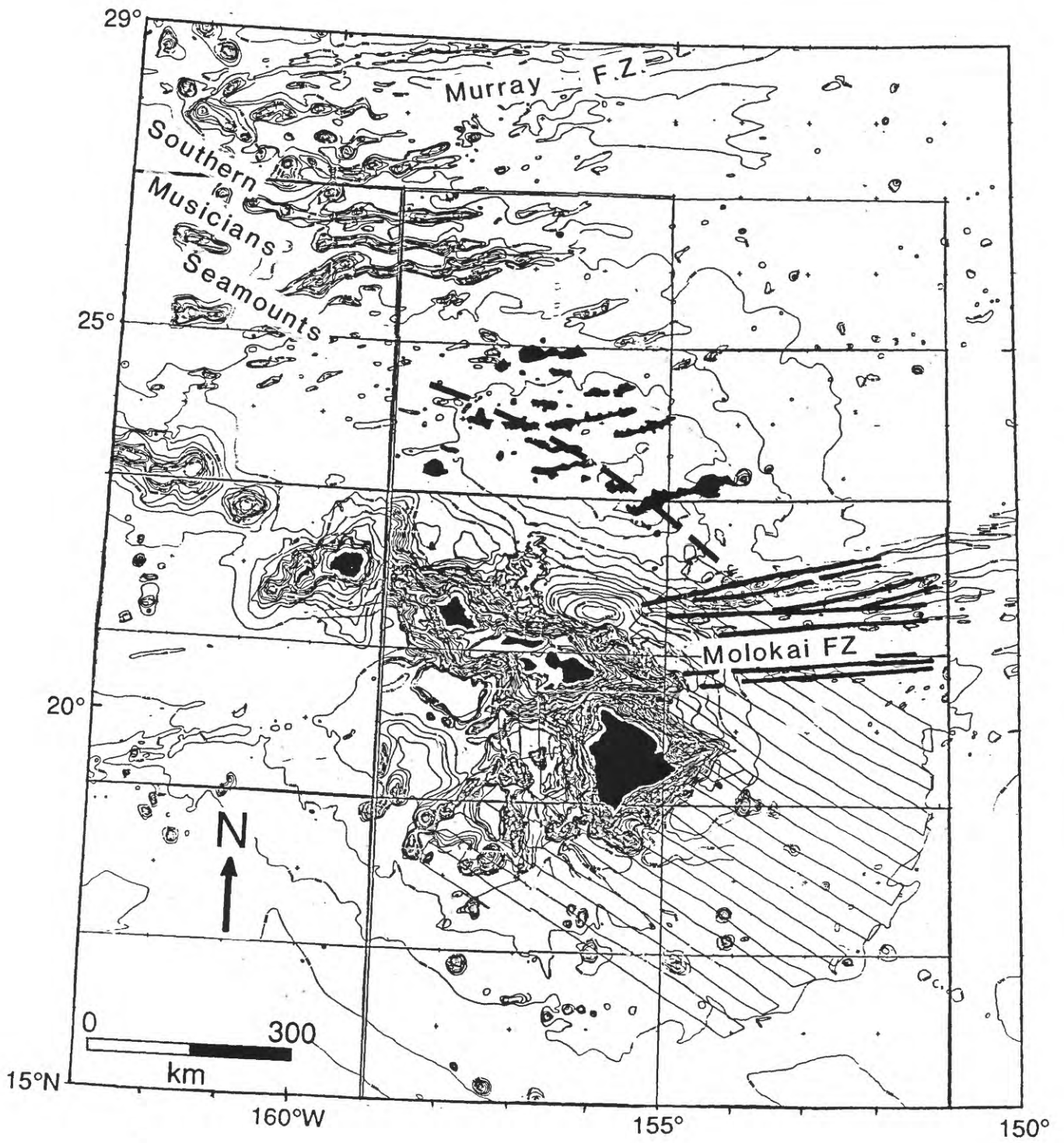
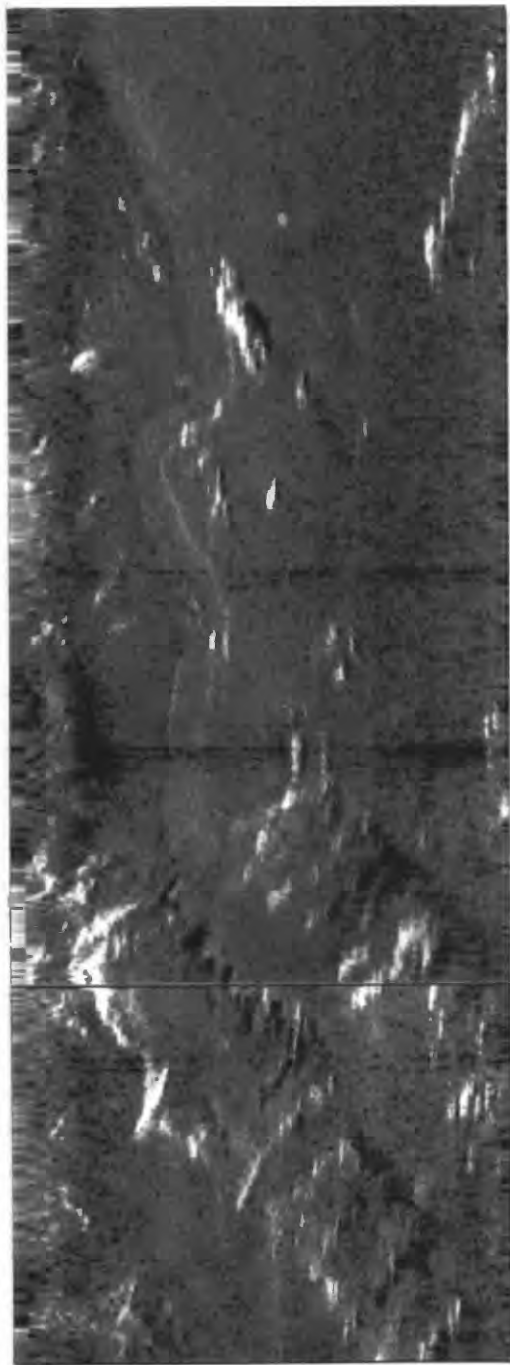
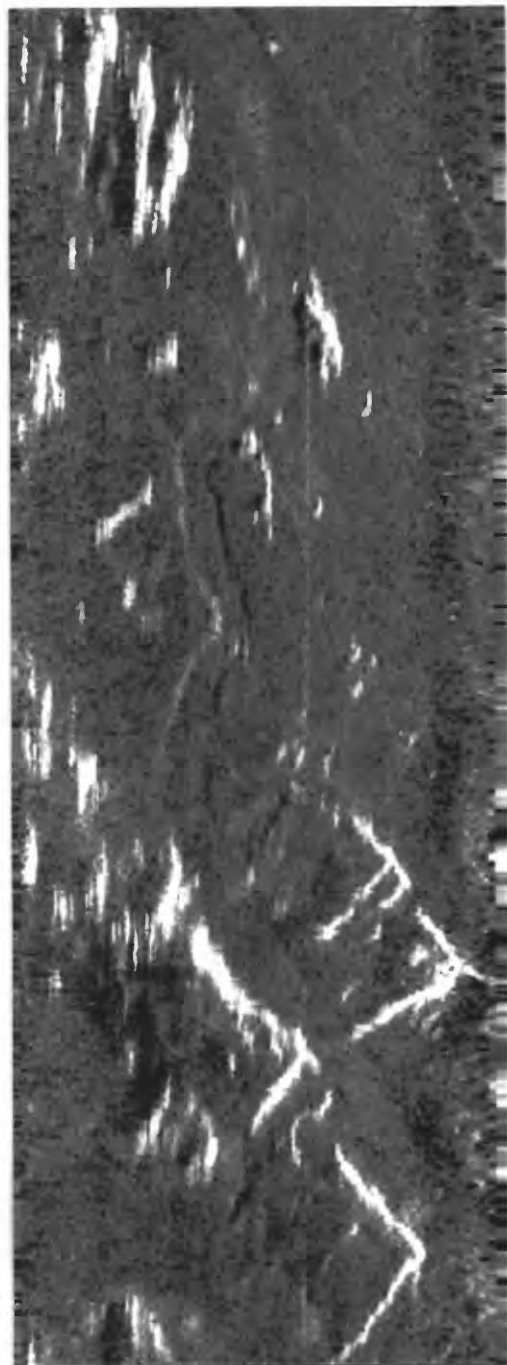


Figure 12



B



A



Figure 13

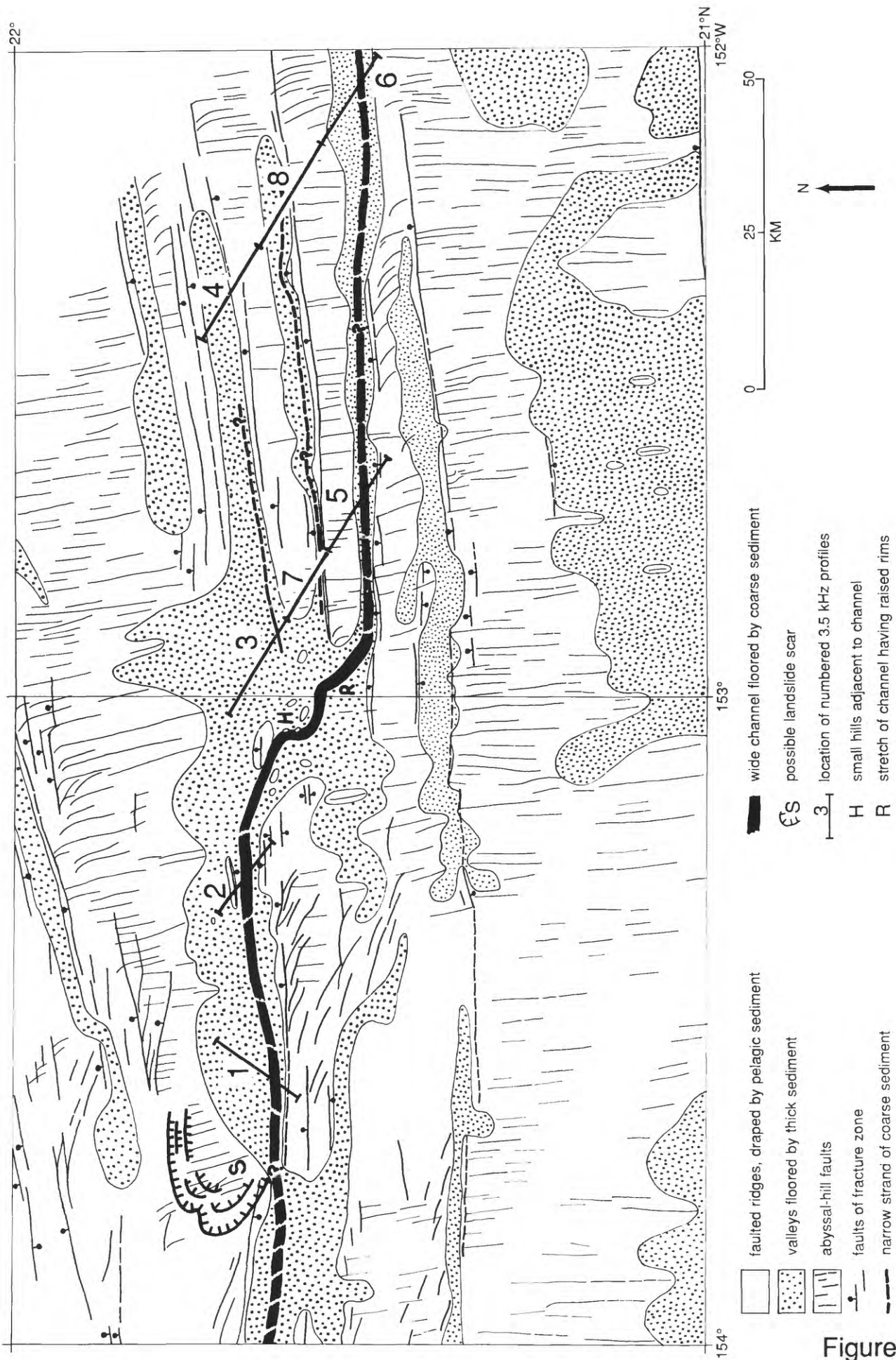


Figure 14

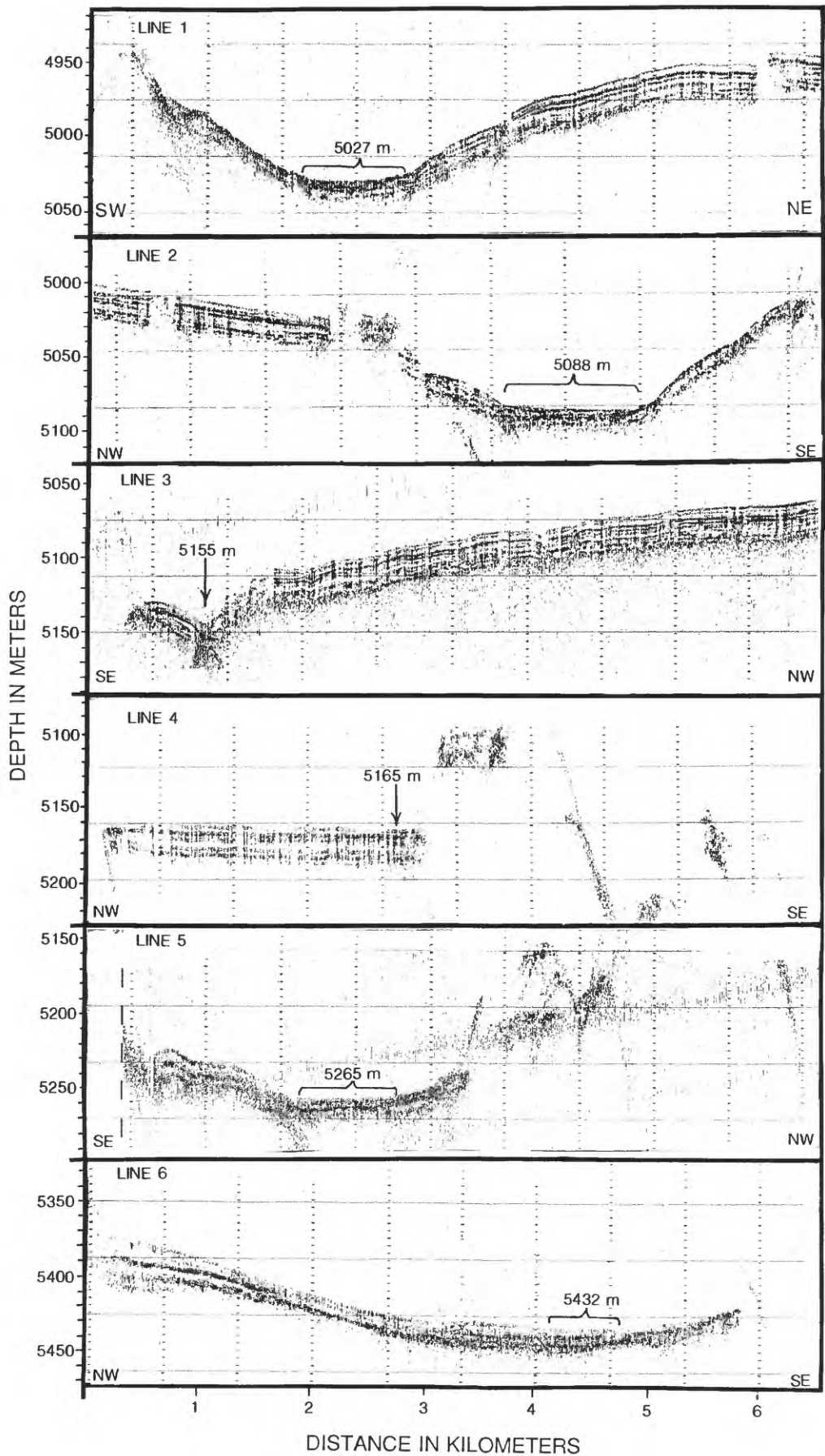


Figure 15

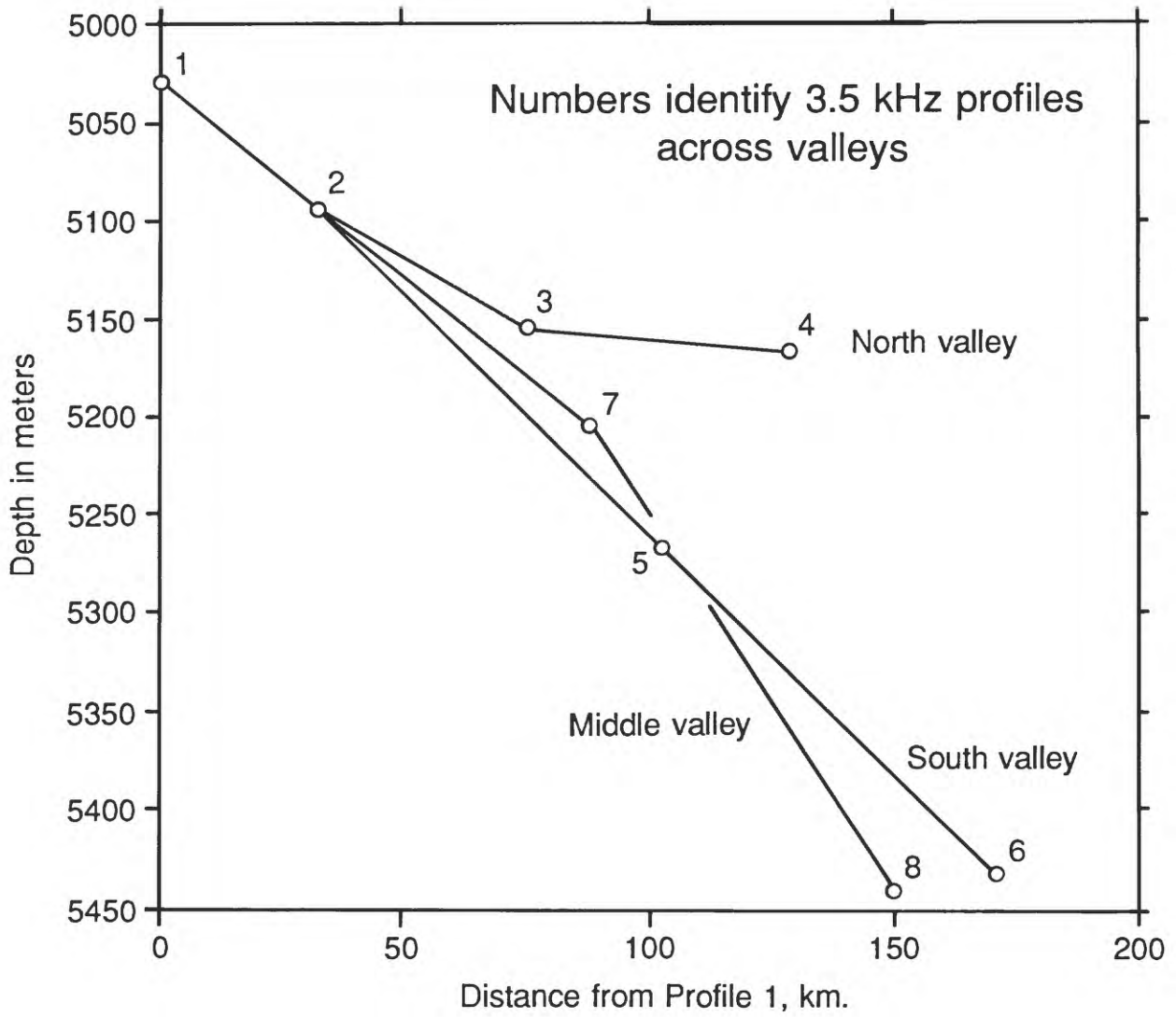


Figure 16

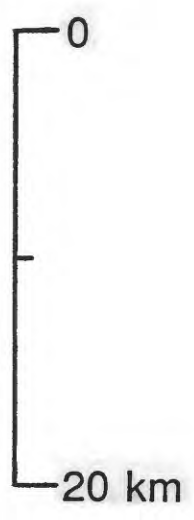


Figure 17

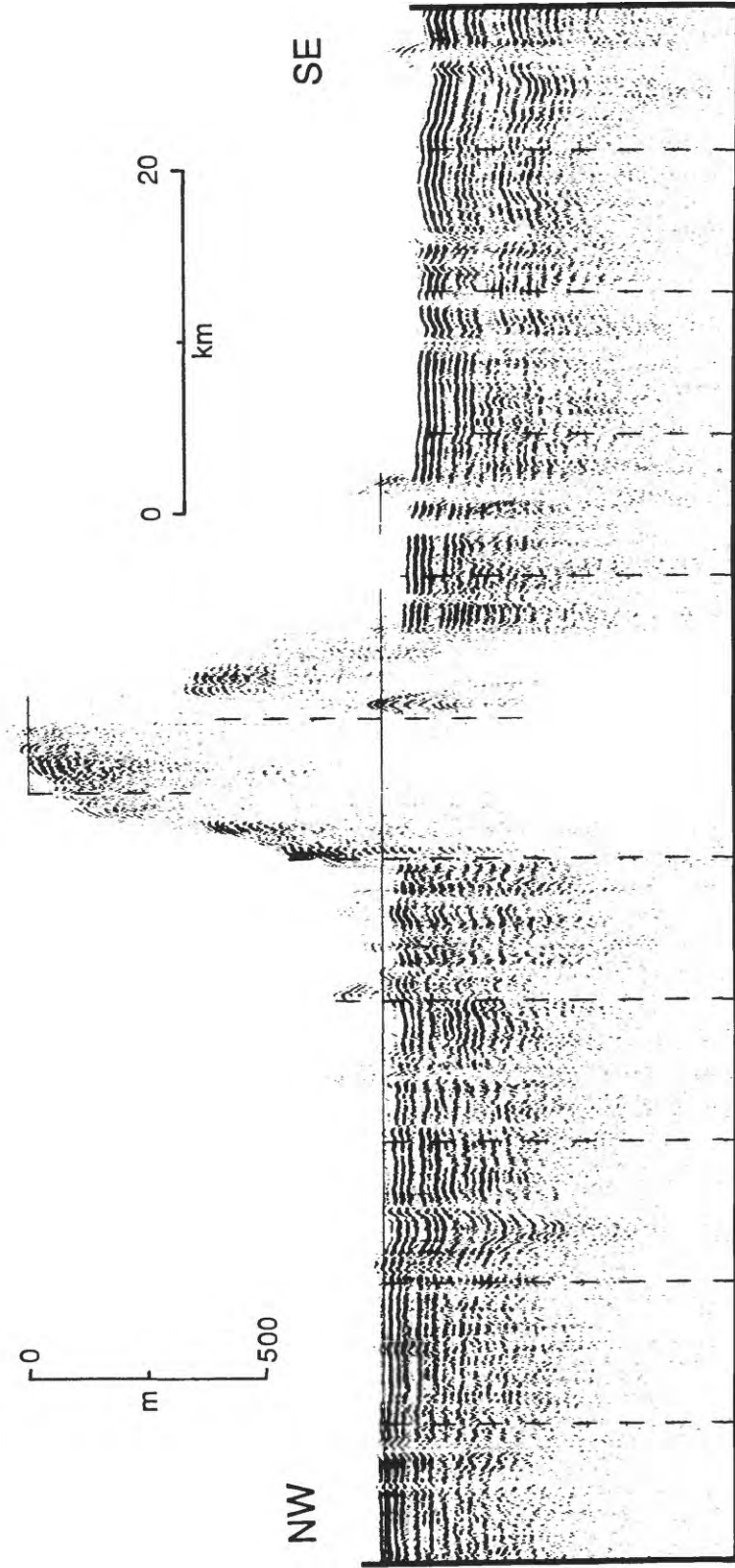


Figure 18

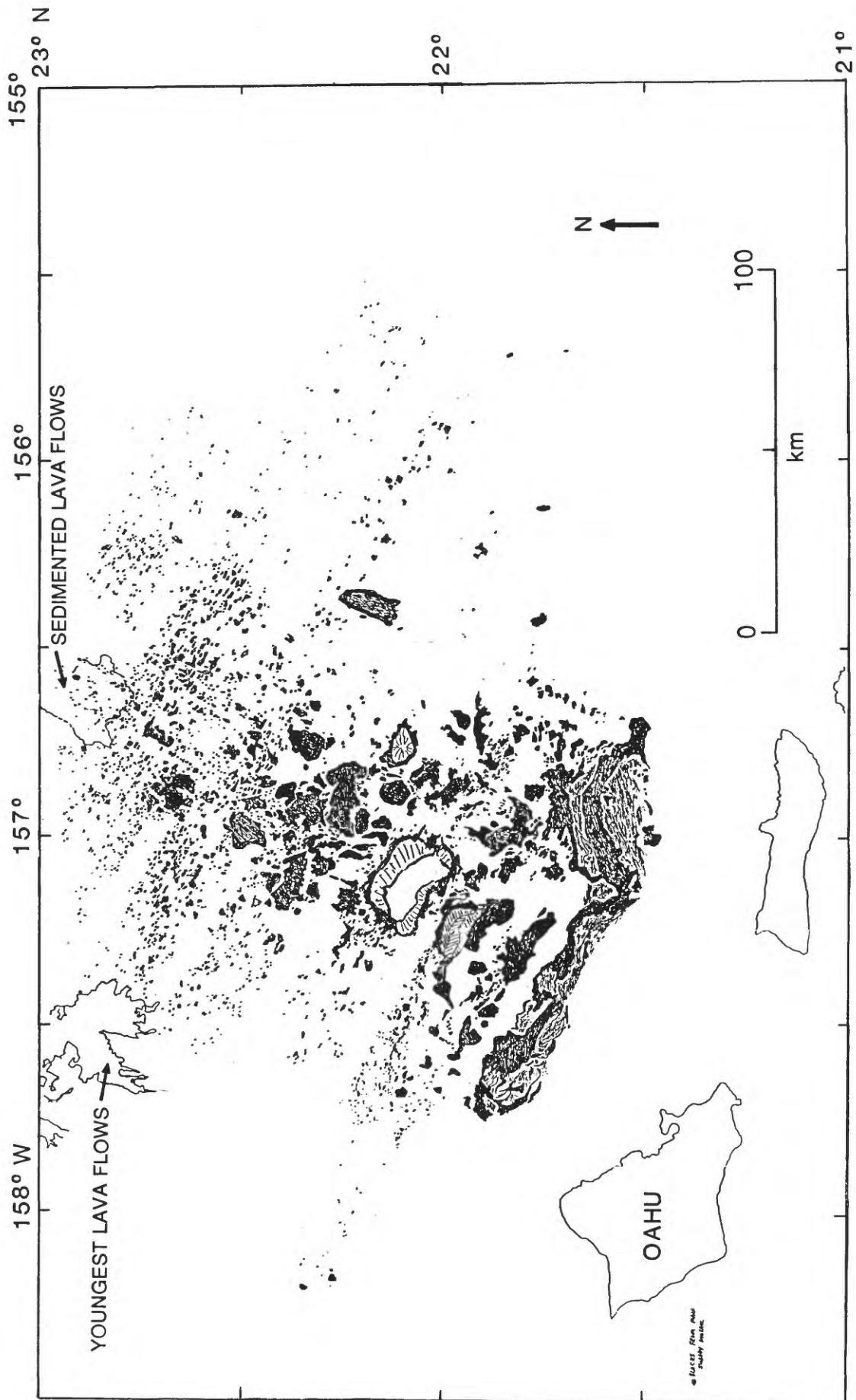


Figure 19

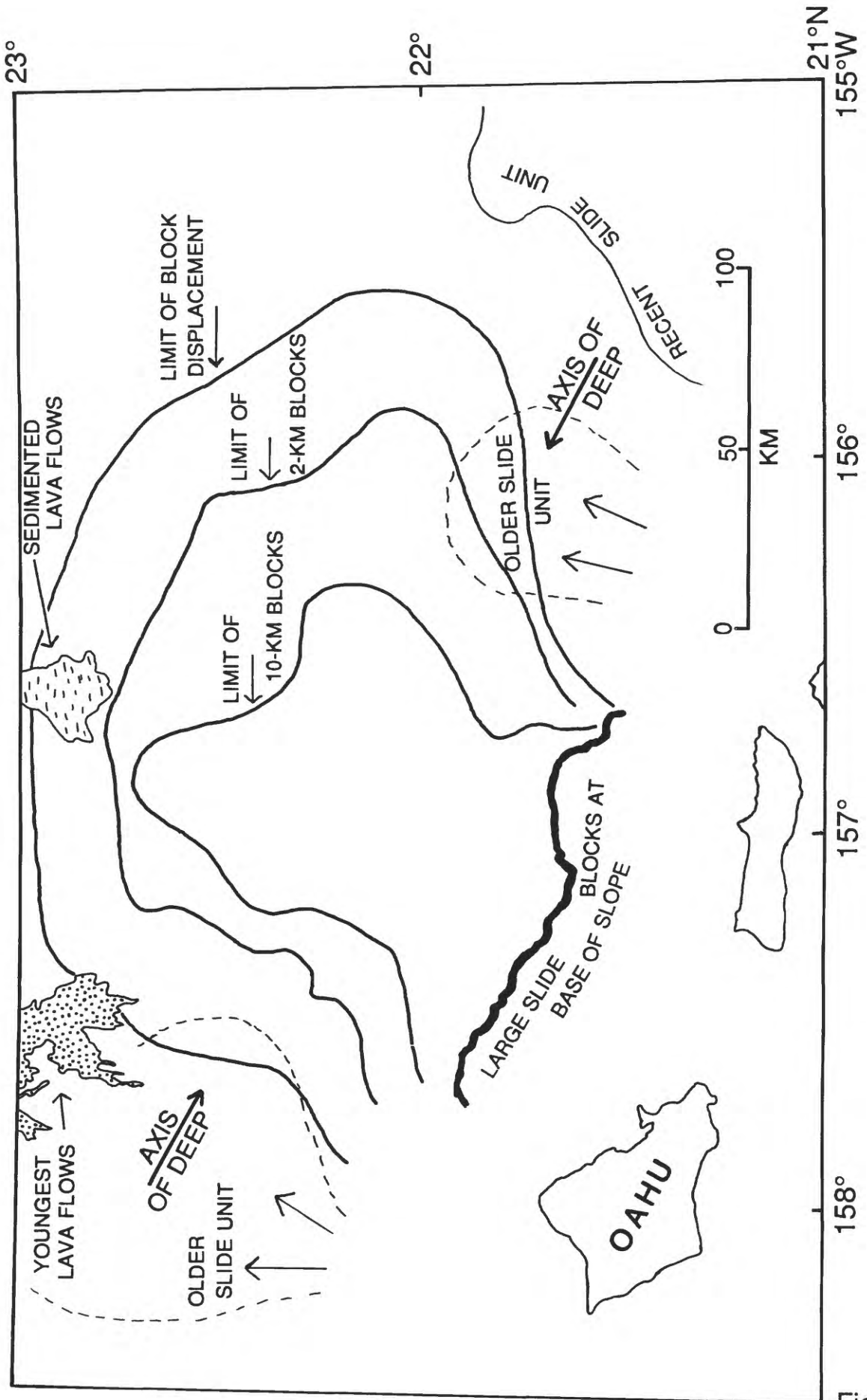


Figure 20